THE PHYSICS OF SPUTTERING

by

B. J. STOCKER, B.Sc., A.R.C.S.

A Dissertation submitted for the M.Sc. Degree
of the University of London

Physics Department,
Northern Polytechnic,
London.

June 1962

CONTENTS

ABSTRACT

Early sputtering observations were made in the abnormal glow discharge at pressures around 1 mm Hg and indicated that the mass sputtered per unit charge passed through the discharge tube varied linearly with the cathode fall of potential. More recently the author has made measurements at pressures around 10 mm Hg and found that the mass sputtered per unit time varies as $\left(\frac{i}{p}\right)^{2.5}$, where i is the current and p is the pressure.

In order to investigate the sputtering process actually occurring at the target bombarded by the ions, measurements have been extended to lower pressures by applying a magnetic field to the glow discharge, by immersing the target as a negative probe in an arc discharge plasma, or by bombarding the target with a positive ion beam. By these methods information has been obtained on the variation of the sputtering yield with ion energy, gas pressure and the angle of incidence of the ions. In addition, the angular distribution of the sputtered material, especially from monocrystalline targets, has been observed, and the sputtered particles shown to consist mainly of high speed neutral atoms. The phenomenon of gas clean-up has been shown to be closely related to sputtering.

A number of theories of sputtering have been proposed. The most satisfactory appear to be those, like that of Langberg, in which the energy of the bombarding ion is considered to be transferred to the sputtered atom by a number of two-body collisions, rather than by local heating of the target surface and evaporation of the atoms. No really satisfactory theory has been proposed for sputtering in the glow discharge.

1. INTRODUCTION

Sputtering is the emission of atoms from a target when bombarded by atoms or ions, especially positive ions in a gas discharge. The majority of the sputtered atoms are normally uncharged, although there may be an ionic component.

The phenomenon of sputtering has been known for more than a century having been observed by Grove[1] in 1852 and Pluecker[2] in 1858. All early observations were of the sputtering by positive ions at the cathode of the abnormal glow discharge. However, it is difficult under these conditions to obtain information about the actual process occurring at the cathode. The reason for this is that the incident ions can have all energies between zero and that corresponding to the cathode fall of potential, and all angles of incidence; the secondary emission coefficient, and hence the actual ion current, is unknown; and the sputtered particles travel through the gas to a collector by a diffusion

process, in which more diffuse back to the cathode than escape. An additional complication is the impossibility of varying the discharge parameters, current, cathode fall and pressure independently of one another.

More recently sputtering measurements have been extended to lower pressures, where the back diffusion of sputtered material can be neglected and the ion energy and current density varied independently, by applying a magnetic field to the glow discharge, by immersing the target as a negative probe in an arc discharge plasma, or by bombarding the target with a positive ion beam. By these methods considerable information has been obtained on the sputtering process at the target, but it still remains difficult to relate this to the more complicated conditions in the glow discharge.

Information on sputtering other than by positive ions is very meagre. Sputtering by neutral or metastable helium atoms was reported by Oliphant[3] and shown to be less than for positive helium ions. Jacob[4] claimed to have observed sputtering of barium, strontium, caesium and sodium by electrons, the material being emitted as positive ions, but this seems unlikely as the electron energies were only a few hundred electron volts. Johnson and Harris[5] showed that fast moving neutralized ions reflected from a glow discharge cathode, or electrons of energy greater than 2Ke, could destroy a sputtered deposit by re-sputtering.

Short surveys on sputtering have been written by Massey and Burhop[6], and Francis[7] and a much more detailed article has been provided by Wehner[8]. This dissertation is primarily concerned with sputtering at energies typical of gas discharges, although information at higher energies will be mentioned.

1.1 Methods of Measuring Sputtering

The fundamental quantity which is measured in sputtering experiments is the sputtering yield (or sputtering ratio) S, the number of sputtered atoms per incident ion. Alternatively, especially in the glow discharge, the mass sputtered per unit charge passed through the discharge tube Q, which is proportional to the yield, or the mass sputtered per unit time (or rate of sputtering) M, which equals the product of Q and the current are sometimes measured. Unfortunately certain authors call the quantities S or Q the rate of sputtering.

In calculating the yield the measured current should be corrected for the secondary emission from the target, which must be subtracted to give the true ion current. As the secondary emission is frequently difficult to measure simultaneously with the yield, this correction is frequently not applied, the results being quoted as $S/1+\gamma$ where γ is the secondary emission coefficient for electrons by ions. However at low energies γ is normally constant and less than 0.2.

The yield or rate of sputtering is normally measured by removing the target and determining the loss in weight. However, this method has the disadvantage that surface impurity layers cannot be sputtered off before the initial target weighing. Apparatus in which the target can be weighed continuously during the sputtering has usually proved to be insensitive.

This problem is avoided if it is the weight increase of an insulating collector which is measured, the collector being protected by a shutter movable under vacuum during the initial sputtering. This method is particularly useful if only a relative measure of the yield is required, but it assumes that nearly every sputtered atom hitting the collector sticks to it. This is only true for high vacuum evaporation above a minimum striking intensity, but Ditchburn[9] showed there is no minimum intensity for the sticking of sputtered cadmium atoms, due to the slow ion bombardment of an insulator in a discharge.

Many other methods have been used to obtain a relative measure of the sputtering yield, the most important being the change in light transmission of a transparent collector during deposition of sputtered material. There are other less common methods which will be described later along with the actual experiments.

2. SPUTTERING IN THE ABNORMAL GLOW DISCHARGE

2.1 Early Sputtering Measurements

Sputtering occurs extremely slowly in the normal glow discharge but is much more rapid in the abnormal glow owing to the increased current density and cathode fall of potential. Measurements on sputtering can be made over a pressure range from about 0.1 to several tens of mm Hg.

Most workers have used gas pressures around 1 mm Hg and have found that the mass sputtered per unit charge passed through the discharge tube Q varies with the cathode fall of potential V according to a relation of the form

$$Q = A(V - V_o) \qquad (1)$$

where A and V_o are constants for any gas-metal combination, although V_o is affected by the condition of the surface and the values obtained have fallen as improved cleanliness has been obtained.

The most detailed measurements have been made by Guentherschulze[10]. Using a silver cathode in hydrogen and plane parallel electrode geometry, he showed that for a cathode fall of 1000 volts at a pressure of 0.72 mm Hg, the product of the mass sputtered per unit charge Q and electrode separation was a constant. The graph

obtained relating these quantities is shown in Fig.1. Then keeping the electrode separation always approximately 1.8 times the dark space, and the current density at $3mA/cm^2$, the pressure was varied over the range 0.33 to 2.18 mm Hg and the mass sputtered, the electrode separation d and the pressure p plotted against cathode fall voltage V as in Fig.2. It will be noticed that the mass sputtered Q varies linearly with voltage as required by equation (1). The product Qpd was proportional to the cathode fall as shown in Fig.3, indicating that a relation of the form

$$Q = \frac{BV}{pd} \qquad (2)$$

is obeyed, where B is a constant. Equation (1), but not (2), was also verified for many other target materials in hydrogen and oxygen.

Guentherschulze also investigated the sputtering of a wire and Fig.4 shows the variation in the mass sputtered with diameter. The decrease in sputtering as the wire is made larger is due mainly to the increase in diffusion of the sputtered silver back to the wire, although a similar though smaller effect occurs at very low gas pressures owing to oblique incidence of the ions (Section 6.3). Guentherschulze and Tollmien[11] showed that with certain target materials the sputtered material which returns to the cathode is deposited as upright microscopic cones with apex angles characteristic of the metal. The effect is particularly marked with Mg, Cd, Zn, Al, Sn, Pb, Sb and Bi.

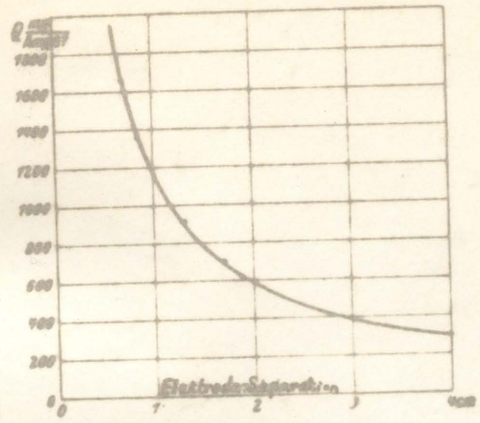

Fig.1. Variation of mass sputtered per unit charge Q with electrode separation.

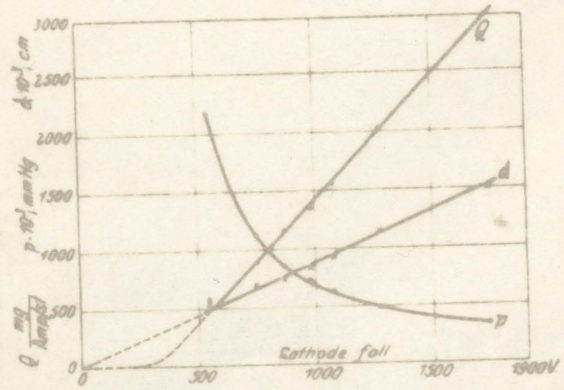

Fig.2. Variation of mass sputtered per unit charge Q, electrode separation d and pressure p with cathode fall voltage.

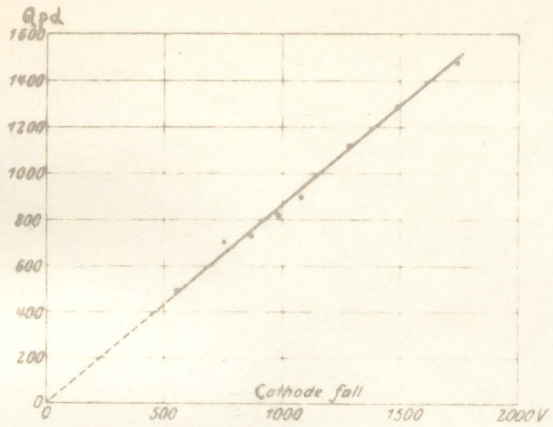

Fig.3. Variation of the product Qpd with cathode fall voltage.

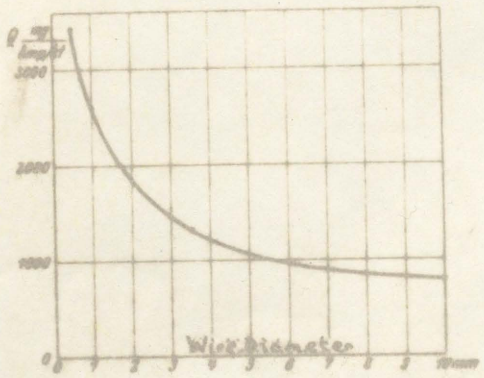

Fig.4. Variation of mass sputtered per unit charge Q with wire diameter.

The presence of the cones increases the probability of a sputtered atom becoming trapped immediately after being emitted, and hence the rate of sputtering decreases with time during the formation of the cones, as shown in Fig.5 for lead sputtered in hydrogen. Also there is often a time lag before sputtering commences which cannot always be explained by an impurity layer.

In later experiments Guentherschulze[12],[13] investigated the distribution of sputtered material deposited on the anode, in a cylindrical discharge tube with plane parallel electrodes extending to the walls. The result is as shown in Fig.6, owing to diffusion of the sputtered material to the tube wall.

Experiments on sputtering in the glow discharge do not normally enable one to measure directly the yield from the cathode which would occur in the absence of diffusion in the gas. Guentherschulze[14] suggested that this problem could be overcome by employing a hollow cathode completely enclosing a small wire anode, serving also as a collector. The anode would collect a negligible fraction of the material compared with the cathode which would therefore receive as much as is sputtered away. An equilibrium presence of sputtered material would be set up and the yield could be determined from the increase in weight of the anode. Unfortunately, this is only true if the collector dimensions are small compared with the mean free path of the sputtered atoms[15] and in Guentherschulze's experiments this condition was not obeyed.

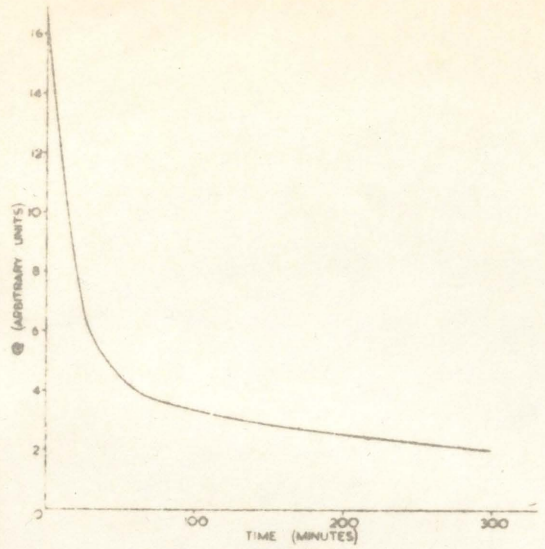

Fig.5. Decrease in sputtering with time, for lead sputtered in hydrogen at 1400V and 0.23 mA/cm^2

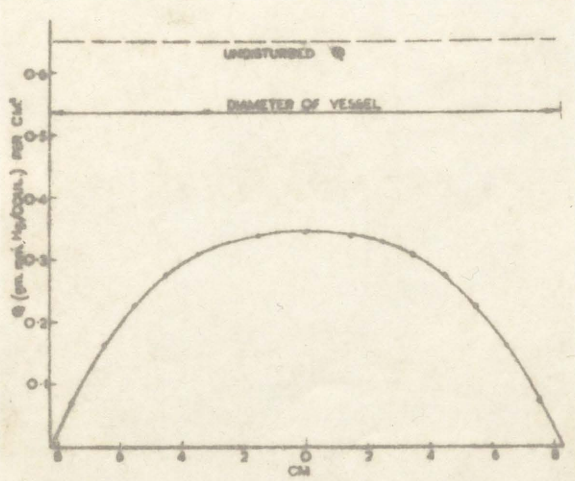

Fig.6. Distribution of sputtered deposits on the anode, for copper sputtered in hydrogen at 875V.

Until recently the only measurements at the upper end of the range of pressures over which sputtering occurs in the glow discharge have been those by Rockwood[16],[17]. He calculated the rate of sputtering from the life-times of some commercial cold cathode tubes. These tubes contained a mixture of 99% neon - 1% argon at 60 mm Hg pressure and had cathodes consisting of a mixture of barium and strontium and their oxides, on a nickel base. During operation this coating was sputtered away and so the life of the tube was determined by the amount of material present and the rate of sputtering. A constant current was passed through each tube until it showed a characteristic rise in voltage, when a large part of the coating had been destroyed, indicating the end of the tube's life. Rockwood showed that his results fitted a theoretical formula by Townes[17] (see Section 10.3). Fig.7, which is taken from the Townes paper, shows the theoretical curve drawn through the experimental points. The sputtering rate was given as 1,000/tube life in hours.

Rockwood also made measurements in pure argon, first at various values of the pressure p but constant $\frac{p^2}{j}$ where j is the current density. The sputtering rate was then found to be proportional to the pressure, as required by the theory. Then at constant pressure the sputtering rate was measured as a function of current, but the agreement with the theory was less satisfactory than for the gas mixture. However, the theory is less accurate in a pure gas than in the mixture, since charge transfer between ions and neutral atoms causes the mean free path to be dependent on the ionic velocity.

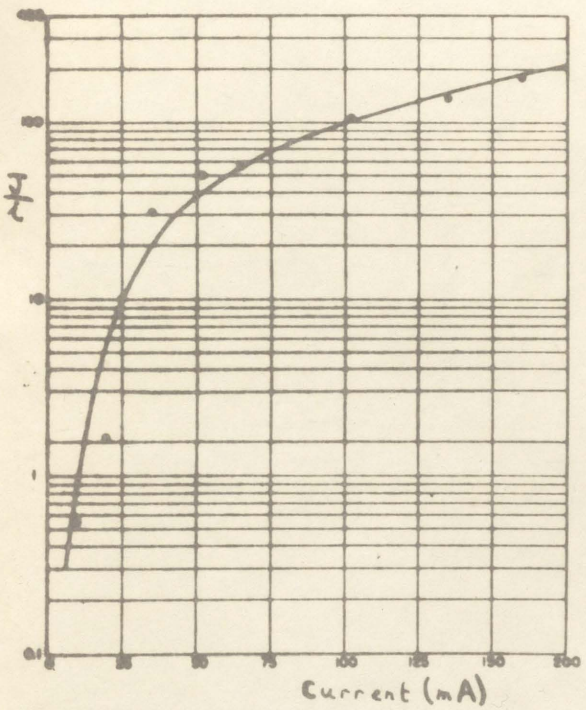

Fig.7. Rate of sputtering per unit current as a function of current i for 99% neon - 1% argon. The equation of the curve is

$$\frac{J}{i} = a\left(7 + 20{\cdot}5/i^{3/5}\right) \exp\left(-20{\cdot}5/i^{3/5}\right)$$

where J is the rate of sputtering measured as 1000/tube life in hours and a is a constant.

2.2 Sputtering Measurements by the Author

Recently the author[18] has made measurements of the rate of deposition of sputtered molybdenum films in inert gases, over the pressure range 3 to 21 mm Hg. The deposition of sputtered material on a glass collector was observed continuously by its optical transmission using a photometer calibrated in terms of optical density D, where $D = \log_{10}\left(\frac{I_0}{I}\right)$ and I_0 and I are the incident and transmitted light intensities.

To determine the relation between the optical density and the mass deposited per unit area, a preliminary experiment was carried out, in which molybdenum was sputtered on to microscope cover glasses in neon, at a pressure of a few mm Hg, in a demountable tube. The optical density of the deposit on a cover glass was determined in the tube, using an internal tungsten filament as light source, the intensity of which was adjusted to correspond to zero density reading before sputtering was commenced. After sputtering, the cover glass was removed and the mass of deposited molybdenum determined by chemical analysis. Exposure to air would not affect this method of measuring the mass. The optical density was found to vary linearly with the mass deposited as can be seen from curve A in Fig.8. Curve B was obtained if the cover slips were removed from the tube for the density measurements, showing the effect of exposure to air. It will be noticed that it is parallel to curve A for thick films.

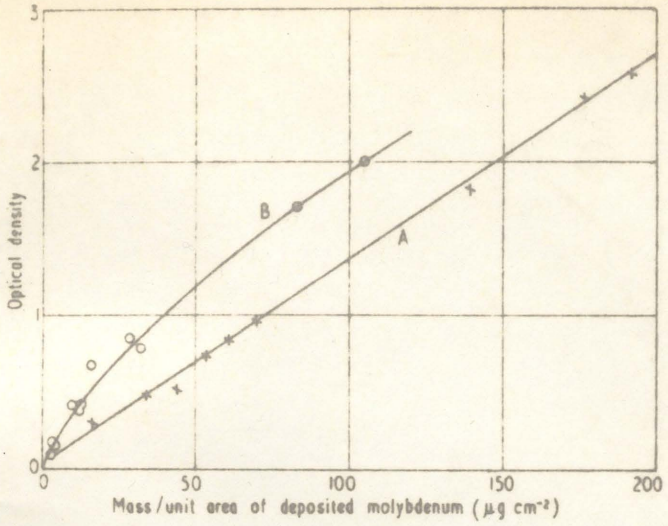

Fig.8. Variation of optical density with mass of molybdenum deposited per unit area.

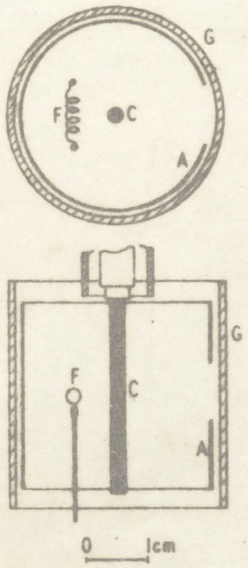

Fig.9. Diagram showing the positions of the anode A, cathode C, filament F and glass collector G in the tube used for measurements of the rate of deposition.

The measurements of the rate of deposition of sputtered material were carried out in a tube with a molybdenum rod cathode C, surrounded by a concentric cylindrical molybdenum anode A (Fig.9). A square aperture was cut in the side of the anode through which particles sputtered from the cathode passed to a cylindrical glass collector G, magnetically rotatable so as to enable a series of deposits to be formed. A tungsten filament F mounted inside the anode cylinder was used as a light source. It was sufficiently intense for the light from the discharge to be negligible by comparison. The filament was electrically isolated from the discharge circuit to prevent it from being sputtered. The tube was sealed to a conventional mercury diffusion pumped system with liquid – oxygen traps, via an Alpert-type bakeable metal tap. It was evacuated and baked to 450°C and the metal parts outgassed at red heat. The cathode was then cleaned by sputtering in inert gas for several hours.

The densitometer was arranged to receive the light from the tungsten filament in the tube via the aperture in the anode, extraneous light being reduced to a minimum. The tube was filled with inert gas at the required pressure and the discharge and filament currents switched on. After allowing the tube to warm up for twenty minutes the gas pressure was measured with a 0 - 25 mm Hg McLeod gauge. The Alpert tap was then closed, thus sealing the tube from sources of contamination in the pump system. The glass collector was rotated to bring an unsputtered portion before the aperture in the anode and the filament

current adjusted to give zero density reading. A series of readings of the optical density of the sputtered deposit and the voltage across the tube, at constant current, was taken at suitable time intervals.

A series of graphs of optical density against time was obtained at various currents and pressures in neon and in the Penning mixture 99% neon - 1% argon. These graphs were normally straight, except for slight initial curvature, and had slopes which were proportional to the rate of deposition since curve A in Fig.8 was linear. These slopes are referred to as the relative sputtering rate since they are assumed to be proportional to the actual rate of sputtering at the cathode.

The sputtering rate $M = Qi$ could not be expressed adequately in terms of the voltage V, current i and pressure p by means of equations (1) or (2) or by the equation of Townes. However, it was found that the sputtering rate could be related to the current and pressure only. Fig.10 shows a series of curves of relative sputtering rate against pressure on logarithmic scales, for different currents, the gas being 99% neon - 1% argon. It will be noticed that a series of parallel straight lines is obtained of negative slope of magnitude about 2.5 Fig.11 for neon is similar and has approximately the same slope. In Fig.12 the rate of sputtering at 10 mm Hg is plotted against current on logarithmic scales, both the 99% neon - 1% argon and the neon points lying on one line of positive slope of about 2.5. Hence the rate of sputtering can be related to the current i and pressure p by an empirical expression

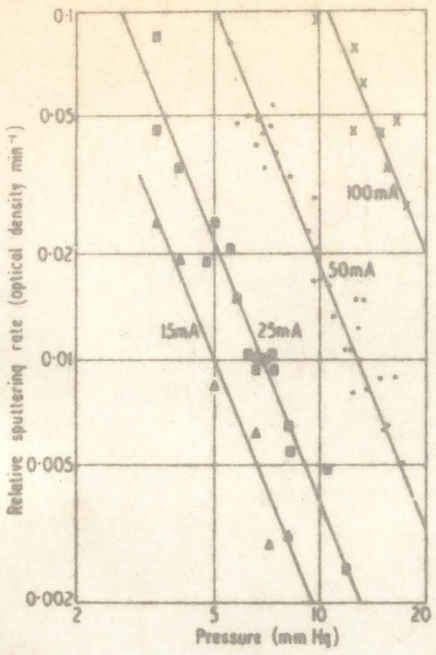

Fig.10. Variation of sputtering rate with pressure for 99% neon - 1% argon.

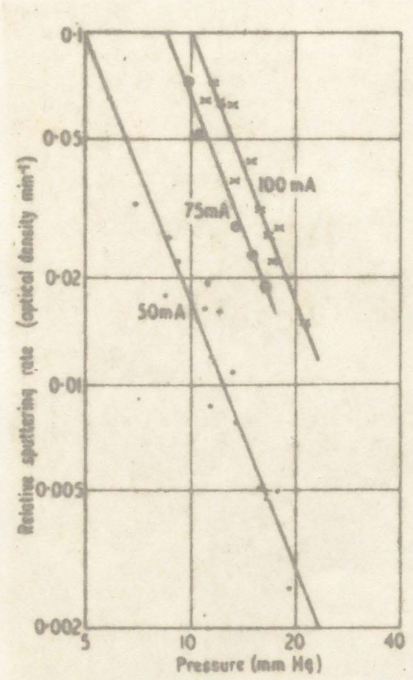

Fig.11. Variation of sputtering rate with pressure for neon.

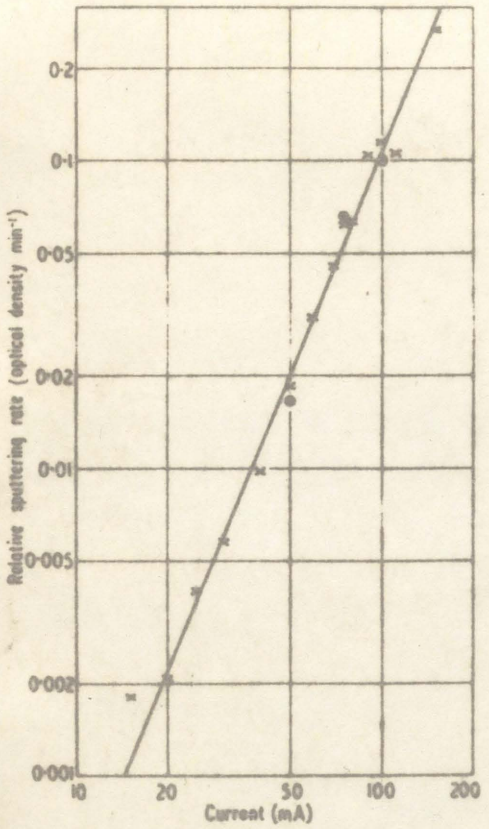

Fig.12. Variation of sputtering rate with current, at a pressure of 10 mm Hg
× 99% neon - 1% argon; • neon.

of the form

$$M = Qi = C\left(\frac{i}{p}\right)^{2.5} \qquad (3)$$

where C is a constant. C is approximately the same for both neon and 99% neon - 1% argon, which is surprising since the majority of the ions in the gas mixture are of argon. However, the lower voltage required in the gas mixture may compensate for the greater mass of the ions.

An attempt was also made to observe sputtering in helium. This proved to be practically negligible, confirming the statement of Guentherschulze[13] that sputtering does not occur in helium up to ion energies of at least 800eV. However the addition of only 0.085% of neon increased the sputtering rate to a value comparable with that in pure neon.

2.3 The Nature of the Material Sputtered in the Glow Discharge

It was shown by von Hippel[19] that when cadmium, zinc or silver were sputtered their resonance spectra were emitted. By comparing the vapour pressure calculated from the amount sputtered in a given time with that estimated by spectroscopic measurements, he showed that most if not all the material is sputtered as atoms. This was confirmed by Baum,[20] for silver sputtered by hydrogen ions, by applying a magnetic field, but it was shown that the atoms could coalesce into aggregates or become

charged under the influence of the discharge and so be deflected by the magnetic field. From the deflection of the ions formed he showed that their velocities were comparable with those of evaporated atoms. However Guentherschulze[12], by observation of the density of sputtered deposits as a function of distance from the cathode, concluded that sputtered atoms are emitted with much higher energies than evaporated atoms.

The spectrum of the sputtered atoms may be quite intense, as shown in Fig.13 which is a spectrograph taken by the author of the negative glow in a neon discharge between molybdenum electrodes, showing the three lines of the unionized molybdenum spectrum at 3798, 3864 and 3903 Angstroms. In the case of a helium discharge no molybdenum lines are emitted, thus confirming the absence of sputtering in helium, as can be seen from Fig.13. In this case the spectrum in the negative glow is mainly the He_2 band spectrum.

When the cathode consists of metals of low ionisation potential like caesium and barium, the sputtering does take place mainly as ions, as is shown by the emitted spectrum. Also as shown by Cayless and Forster-Brown[21] using barium, the sputtered material is not deposited as a diffuse area covering most of the discharge tube wall, but as highly localised spots with quite sharp boundaries. This is explained as being due to regions of different work function on the wall receiving different numbers of sputtered ions. If there are two regions of wall of work

Fig.13. Spectrograph showing the presence of molybdenum lines in the spectrum of the negative glow in neon, but not in helium.

functions ϕ_1 and ϕ_2 to which the ion current densities (and also the electron current densities) are j_1 and j_2 and where the plasma densities are n_1 and n_2, then

$$\frac{j_2}{j_1} = \frac{n_2 \exp\left[-e(V+\phi_2)/kT_e\right]}{n_1 \exp\left[-e(V+\phi_1)/kT_e\right]} = \frac{n_2}{n_1} \exp\left[\frac{e(\phi_1-\phi_2)}{kT_e}\right]$$

where V is the potential of the plasma above the wall, T_e the electron temperature, $-e$ the electronic charge and k is Boltzmann's constant. Hence regions of lower work function receive more sputtered material than those of higher work function. This results in a further lowering of the work function in these regions and hence the effect is cumulative.

2.4 Chemical Sputtering

This is a completely different sputtering process which was found by Guentherschulze[22] to occur in the sputtering of carbon, selenium, tellurium, arsenic, antimony and bismuth by hydrogen. It can also occur with certain metals sputtered by oxygen or nitrogen. Unlike ordinary physical sputtering, where the thickest deposit forms on the tube wall nearest the cathode, in chemical sputtering it occurs further away from it. Chemical sputtering can occur at negligibly small ion energy, and does not vary appreciably with ion energy. Hence it can also occur at any insulator in the discharge and at the anode. The explanation of the phenomenon is the formation of volatile metal-hydrogen

(or oxygen, etc.) compounds which decompose and deposit metal on the tube walls. Small traces of hydrogen in another gas can cause this phenomenon since the hydrogen is not lost in the process.

2.5 Applications of Sputtering in the Glow Discharge

Sputtering was used soon after its discovery as a means of producing thin layers of metal. However, for most metals evaporation in a vacuum is now preferred for this purpose as the films produced are free of gas, sputtering only being used for metals which require an impracticably high temperature to give the required vapour pressure. However, chemical or "reactive" sputtering has recently become important for producing metal oxide conducting films by sputtering in argon-oxygen mixtures, as suggested by Holland and Siddall[23].

Sputtering at pressures around 20 mm Hg is of considerable importance in the production of glow discharges of stable and reproducible cathode fall as suggested by Jurriaanse, Penning and Moubis[24],[25]. The effect of the sputtering is to remove any impurity from the surface of the cathode and deposit it on the glass wall, and the pure metal which is deposited once the cathode is clean serves as a getter to remove impurity from the gas and to prevent the discharge releasing contaminant from the glass. This process is most effective in the case of molybdenum electrodes in inert gases. By this method Jurriaanse et al.[25] were able to obtain reproducible values

for the normal cathode fall for molybdenum and zirconium in various inert gases and their mixtures, and Penning and Moubis[26] values for various metals in neon. This has had considerable commercial importance in the production of stabiliser and voltage reference tubes[27].

McCutcheon[28] has suggested the use of sputtering in a glow discharge in 20μ of argon as a means of etching metal surfaces and this has recently proved to be of some importance.

Frequently it is necessary to reduce sputtering to a minimum, as in glow discharge indicator lamps where a sputtered deposit on the glass will reduce the light output and may eventually result in short-circuiting of the electrodes. One method of achieving this is to use aluminium or magnesium for the electrode materials[13]. Although the metals themselves sputter readily, a thin oxide layer on the surface reduces the sputtering to a very small amount. The addition of a trace of oxygen or water vapour to the inert gas filling serves to renew the slowly sputtered oxide layer. An alternative method is to use very pure helium as the filling gas, but the least trace of any impurity will allow sputtering to occur.

2.6 Conclusion

Since the sputtering process in the glow discharge is so complicated, many experiments have been carried out under simpler

conditions at lower pressures, and will be described in the succeeding sections. Theories of sputtering in the glow discharge will not be considered until after the low pressure sputtering experiments and theories.

3. SPUTTERING IN THE GLOW DISCHARGE WITH A MAGNETIC FIELD, AT LOW PRESSURES

This method of observing sputtering was used by Penning and Moubis[29] and enabled them to extend glow discharge measurements to lower pressures, thus reducing the back diffusion of sputtered material and making the mean ion energy more equal to the voltage across the tube than in the ordinary glow discharge. The effect of the magnetic field was to increase the length of the electron paths by causing the electrons to move in spirals, thereby increasing the ionisation produced. The field also served to return many of the secondary electrons to the cathode, thus making the measured current more equal to the sputtering ion current. By varying the magnetic field, the discharge voltage and current, and the pressure could be varied independently of each other.

The apparatus used consisted of a cylindrical water-cooled cathode surrounded at the ends by anode rings, the magnetic field being parallel to the cathode. The cathode was made of copper or aluminium, or copper plated with nickel or silver and the measurements were carried out in argon and hydrogen.

The sputtering yield was determined from the weight increase of small mica plates, which could be moved by a magnet outside the discharge tube and successively exposed to the sputtered particles without opening the tube.

The most extensive measurements were for copper in argon and extended over the pressure range 0.003 to 0.3 mm Hg, the voltage range 400 to 1400volts and the current range 0.5 to 3.5 amps. After correction for the secondary emission coefficient γ the sputtering yield was found to be roughly proportional to the voltage, but to decrease slightly with increasing current. This latter result is surprising and has not been confirmed by sputtering experiments using other methods. It has been explained by Wehner[8] as being due to the decreasing probability for oblique angle impacts, since the ratio of the cathode fall thickness to the ionic mean free path decreases as the ion current density increases. The yield showed a maximum with pressure at about 0.02 mm Hg. Penning and Moubis suggested that the decrease in yield at lower pressures was due to the electrons being liberated mainly from the ends of the cathode, giving the discharge an abnormal character. Wehner[8] again gives an explanation based on the variation of yield with angle of incidence. He suggests that below 0.01 mm the incidence was normal and the yield constant, between 0.01 and 0.02 mm the yield increased due to the increasing number of obliquely bombarding ions and above 0.02 mm the yield decreased due to the decreasing average ion energy and increasing back diffusion of sputtered atoms.

Although the accuracy in these measurements was poor (Penning and Moubis estimated it as 25% for copper in argon) the experiment is interesting as the pressure range covered extends from that used in

glow discharge measurements to pressures typical of measurements in arc discharges, as described in the next section. There have been no attempts by other workers to make sputtering measurements by this method.

4. OTHER METHODS OF OBSERVING SPUTTERING AT LOW PRESSURES

4.1 Sputtering of Probes in Arc Discharge Plasmas

By reducing the pressure in the discharge tube to about 1 micron, the problems of diffusion of the sputtered atoms, and the indeterminate energy of the ions bombarding the target, are eliminated, since the mean free paths of the ions and the sputtered atoms become greater than the tube dimensions. Since a glow discharge will not operate at this pressure (except in the presence of a magnetic field as described in the previous section) the discharge must be an arc with a thermionic or mercury pool cathode. The target is immersed in the plasma produced, as a negative Langmuir probe, and is bombarded by ions all of which have the energy corresponding to the potential difference V between the target and the plasma (which is approximately at the anode potential of the arc).

The target is surrounded by a dark sheath, the Langmuir dark space, of thickness d_c, which for a plane target is related to the ion current density j_+ and the potential difference V between the target and plasma by the Langmuir-Child equation (in e.s.u)

$$j_+ = \left(\frac{2e}{m}\right)^{\frac{1}{2}} \frac{V^{\frac{3}{2}}}{9\pi d_c^{\,2}} \qquad (4)$$

where e is the charge and m the mass of the ions. Positive ions whose thermal motion carries them to the sheath edge are attracted to the target.

Hence the ion current is given by the relation

$$j_+ = \frac{N_+ e c_+}{4} \qquad (5)$$

where N_+ is the positive ion density in the plasma near the sheath and c_+ is the mean thermal speed of the ions. The ion density N_+ is determined by the arc current. Hence, unlike measurements in the glow discharge, the ion current density j_+, given by equation (5), can be controlled independently of the ion energy, which is determined by the potential applied between the target and anode. At low energies (below 100eV) a correction is made by probe measurements for the potential difference between the plasma and anode and also for the contact potential difference due to different anode and target work functions. For a plane target, large compared with d_c, the bombardment is perpendicular to the surface, but for smaller targets oblique bombardment occurs. It is not normally possible to measure the secondary emission coefficient γ and so the yield must be expressed as $\frac{S}{1+\gamma}$, as explained in section 1.1.

There have been very many experiments using this method, which will be described in more detail in later sections where the variation of yield with energy, current density, gas pressure, angle of incidence, etc. will be considered separately.

4.2 Sputtering by Ion Beams

Sputtering measurements can be made by bombarding a target with a monoenergetic ion beam in a high vacuum. This has the advantage over the method described in the previous section that the angle of incidence can be more easily varied and the secondary electron current from the target can be collected by a suitable electrode or returned to the target, allowing the yield (S) as distinct from $\frac{S}{1+\gamma}$ to be determined. However, the ion current densities obtainable are much smaller than for a probe immersed in a plasma (about 10 $\mu A/cm^2$ compared with 10 mA/cm^2). This results in longer sputtering times and the greater risk of contamination of the target by impurities in spite of the lower pressures, than for the probe method. The ion beam method is more suitable for measurements at high energies, the probe method being better at lower energies (i.e. up to a few hundreds of eV). As with the probe method, the individual experiments will be described in later sections.

5. THE VARIATION OF SPUTTERING YIELD WITH ION ENERGY, FOR NORMALLY INCIDENT IONS

5.1 Early Yield Measurements in Arc Discharges

Among the earliest yield measurements in arc discharge plasmas were those carried out at the laboratories of the General Electric Company, London[30]. The target was in the form of a tungsten filament wound into a helix and the loss of material during sputtering was measured as a change in resistance. Unfortunately the use of a helix causes large differences in the angles of incidence of the ions and also results in a high proportion of the sputtered atoms returning to some part of the wire. The ion current density was small (less than 5 $\mu A/cm^2$) making the sheath thickness of the order of the tube dimensions, again causing the angle of incidence, and also the ion energy to be indeterminate. The low current density could also result in the formation of surface impurity layers on the target during the sputtering. The gases investigated were as follows, in order of increasing rate of sputtering: hydrogen, helium, nitrogen, neon, mercury vapour and argon. The sputtering yields increased linearly with ion energy.

Kingdon and Langmuir[31] observed the sputtering of a monolayer of thorium from a tungsten filament by the decrease in thermionic emission, the emission from thorium being 10^5 times higher than from tungsten. The method was very sensitive since a monolayer

is equivalent to a tenth of a microgram per square centimetre. However, as with the G.E.C. measurements, the ion current density was small. The tube used had a straight thoriated tungsten filament, centrally mounted between two parallel tungsten filaments, and the walls were coated with tungsten evaporated from the outer filaments. The outer filaments were heated so as to emit electrons which were collected by the tungsten layer on the walls of the tube. The electron current produced ions in the filling gas which were accelerated to the cold central filament. This filament was heated when it was required to determine the amount of thorium sputtered.

The ions used to bombard the filament, in order of increasing sputtering, were hydrogen (no sputtering at all, even at 600 volts) helium, neon, mercury, and argon and caesium. The sputtering did not proceed at a uniform rate being greater when 0.95 of the surface was covered with thorium than when it was completely covered. The suggested explanation was that the removal of thorium took place mainly round the edges of holes or depressions in the thorium coating. For the removal of the first few atoms, two successive impacts on the same thorium atom were necessary. The first impact depressed the atom from the surface while at the second impact the ion was reflected from this depressed atom and knocked off one of the surrounding atoms. A different mechanism must apply to the slow sputtering in helium.

Much more satisfactory conditions were present in the experiments of Guentherschulze and Meyer[32]. An arc discharge of several amperes was produced between an oxide cathode and a cylindrical anode which surrounded it, at gas pressures below ten microns. Ions were pulled out of the discharge and accelerated to a sputtering target, in the form of a disc of 5 cm diameter, 2.5 cm from the cathode. The target was suspended from a spring balance. The plasma density was so high that an ion current density of about 1 mA/cm^2 was obtained, and with a sheath thickness at 1,000 volts energy of the order of 5 mm, essentially normal bombardment of the target occurred. The use of a spring balance in the tube enabled surface layers to be sputtered off before measurements were commenced, but the sensitivity of the balance was not sufficient for adequate measurements near the sputtering threshold. For this reason the balance was dispensed with in later experiments by Meyer and Guentherschulze[33], the tube then being broken open to enable the target to be weighed. In the earlier experiments sputtering measurements were made for copper and silver targets in helium, hydrogen, nitrogen, neon and argon, and in the later experiments for sixteen metals in mercury vapour, the vapour pressure being controlled by the temperature of an oil bath surrounding the tube.

No sputtering was detected in helium, at all events up to 800V. In the other gases curves of the mass sputtered per unit charge, Q, against ion energy were plotted, but only for the case of copper in argon was the effect of secondary emission on the measured current

determined. More recently, Guentherschulze[13] has found that all these early results can be related more satisfactorily to the velocity of the ions (or the square root of the energy). In all cases graphs of Q against the velocity of the ions were linear, as in Fig.14 for tantalum in mercury vapour. Hence, assuming the secondary emission coefficient to be constant, the yield was related to the velocity of the ions v by an equation of the form

$$S = A(v - v_0) \qquad (6)$$

where A and v_0 are constants. For the eight metals Al, Si, Mn, Fe, Zr, Mo, Ta and W in mercury vapour the constants in equation (6) are the same, the equation becoming

$$S = 0.0629(v - 13.3) \qquad (6a)$$

the velocity of the ions (v) being in Km/sec. Eight further metals in mercury vapour showed greater yields, the sputtering increasing with the tendency towards amalgamation. For these metals the measurements were only made at 1000 eV energy.

The measurements here described were the earliest upon which any reliability can be placed, but except for copper in argon, no allowance has been made for the current due to secondary emission from the target.

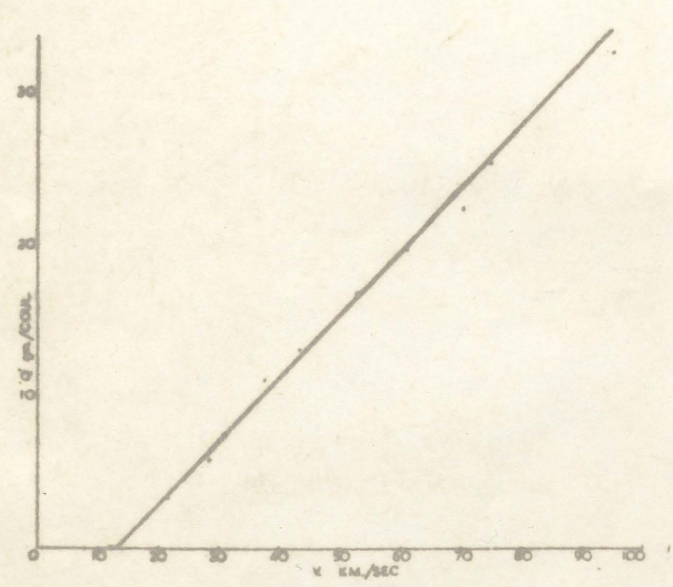

Fig.14. Mass sputtered per unit charge Q as a function of ion velocity v for tantalum sputtered by mercury ions.

5.2 Yield Measurements in Arc Discharges by Wehner et al.

Measurements at low ion energies have been made by Wehner and Medicus[34], by a method based on the change in characteristic of a Langmuir probe when material is deposited on it to change the work function. The apparatus consisted of a demountable, bakeable tube with a tungsten cathode capable of emitting a current of about one ampere, surrounded by a coaxial anode cylinder which also enclosed a platinum target and a movable spherical tungsten probe. Xenon was admitted through a bakeable valve. The probe was cleaned by heating to 2000°C by electron bombardment and its characteristic recorded using an X-Y plotter. The platinum target was sputtered and the probe characteristic again recorded. The change in work function due to the platinum deposited on the probe resulted in a shift of the characteristic along the voltage axis. The time required for a given change in work function was assumed to be inversely proportional to the sputtering rate. By this means sputtering measurements were obtained for bombarding energies of from 40 to 200 eV. The energy range was extended down to 30 eV by observation of changes in the shape of the probe characteristic near plasma potential probably due to changes in the reflection coefficient for slow electrons.

The measurements, which were only carried out for platinum in xenon, showed that at low energies $\frac{S}{1+\gamma}$ was roughly related to the ion

energy (V) by a relation of the form

$$\frac{S}{1+\gamma} = C(V-V_o)^2$$

or for constant γ,

$$S = S_o(V-V_o)^2 \qquad (7)$$

where V_o = 40 eV and C and S_o are constants.

This method of measuring sputtering suffered from the disadvantages that only one side of the probe was exposed to the sputtered platinum and a reliable calibration between the work-function change and amount sputtered could not be obtained. Also the probe characteristic was liable to "creep" along the voltage axis due to the formation of surface impurity layers. However the method was sufficiently sensitive for measurements to be possible at low energies.

More recently sputtering measurements have been made by Wehner[35],[36],[37] using a demountable pool-type mercury arc discharge tube as the source of ions. This type of discharge tube has many advantages as no processing of the cathode is required and the tube can be connected directly to a mercury diffusion pump without a cold trap, thus ensuring pure conditions. Also no difficulties due to gas clean-up can occur (see section 9.2) and the gas pressure can be controlled

by temperature. The plasma density was increased by inserting a fine mesh graphite grid between anode and cathode. This caused the discharge to have an increased voltage drop, which was localised within an electrical double layer in or near the grid holes. Electrons reaching this layer from the cathode were accelerated towards the anode giving increased ionisation. The energy of the accelerated electrons could be controlled by the grid potential and was usually around 40 eV where doubly charged ions were unlikely to be formed. The plasma density was further increased by a negative electrode which repelled the electrons back towards the plasma before collection by the anode, and by applying a magnetic field. Plasma densities of 10^{11} to 10^{12} per cm^3 were achieved at pressures of about one micron and discharge currents of about one ampere.

Sputtered material, from a target immersed in the plasma, passed through a slit in a cylindrical opaque shade to a surrounding cylindrical glass collector[35]. This collector could be rotated magnetically so that many exposures could be made to the sputtered particles without opening the tube. The sputtering yield in relative units could be found from the decrease in the light from the discharge by an external photocell. In later experiments[36] the glass cylinder was replaced by a movable glass ribbon and a tungsten filament light source was used, the discharge radiation being filtered out. Absolute yield measurements were obtained from the weight loss of the target, but no attempt was made to allow for the effect of secondary

emission. To prevent condensation of mercury on the target, the latter was heated to above 300°C.

The initial measurements were approximate determinations of the "threshold" energies for sputtering of 26 metals, by forming sputtered deposits at a series of ion energies at 10 eV intervals. Below a certain ion energy, usually between 50 and 150 eV, the deposits did not occur, indicating the threshold energy. It was found[35],[38] that the product of the momentum transferred to the target atoms at the threshold and the bulk sound velocity of the metal was proportional to the heat of sublimation. In terms of the threshold energy (V_o) the relation is

$$V_o = \left(\frac{1.7 \times 10^5 (m+M) H}{m^{1/2} M v_s} \right)^2 \qquad (8)$$

where V_o is in eV, m and M are the atomic weights of the ion and metal respectively, v_s is the bulk sound velocity of the target metal in cm/sec and H is the heat of sublimation of the metal in Kcal/mole. There is a slight discrepancy between the original letter[38] in which this was reported and a later more extensive article[35] regarding the values of V_o. In the former case the difference between the ionisation potential of the gas V_i and the work function of the metal ϕ is added to the measured values of V_o, on the assumption that the potential energy which becomes available on neutralization of an ion can contribute to the sputtering. This was later[35] considered unlikely as the

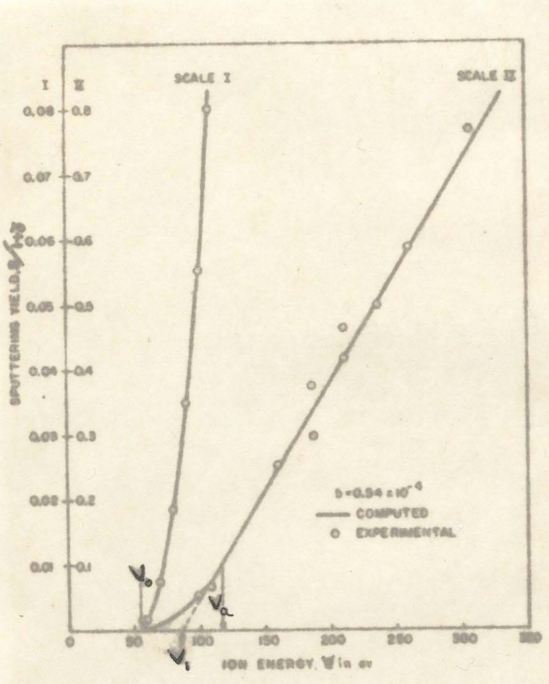

Fig.15. Variation of sputtering yield with ion energy for platinum sputtered by mercury ions. The curve is plotted from Langberg's theoretical equations (20) which are effectively equation (7) below 116 eV and equation (9) above 116 eV.

determinations of the "threshold" energies [redacted] can be roughly identified with the "cut-in" energies V_1 in equation (9), but this has been queried by Henschke[40], who considers that the "thresholds" correspond with V_o in equation (7).

The recently determined values of the "cut-in" energies have not been related to the sound velocity by the empirical threshold relation (equation (8)) but have been shown to obey roughly the relation

$$V_1 \simeq B \frac{H}{\eta} \qquad (10)$$

where H is the heat of sublimation and η is the energy transfer factor at a collision between an ion and a target atom (I.e. $\eta = \frac{4mM}{(m+M)^2}$ where m and M are the atomic weights of the ion and target metal). Some experiments of Laegreid, Wehner and Meckel[41], using germanium targets in thermionic arc discharges in the inert gases, have shown the above rough relation to be expressed better as

$$V_1 \simeq B' \frac{H m^{\frac{1}{2}}}{\eta} \qquad (11)$$

Recently sputtering yield measurements have been extended by Laegreid and Wehner[42] to 28 metals and semiconductors in argon and neon. The yield curves obtained showed only very limited linear portions, the slopes decreasing with increasing energy. The results of

the yield measurements were expressed in tabular form and are reproduced in Table 1, which has been extended to include Wehner's mercury results.

Wehner has shown that if the yield at the same ion energy for a given ion is plotted against the atomic number of the target element, the yield increases in any one period of the periodic table with the increased filling of the d shells; copper, silver and gold giving the highest yields. This is shown in Fig.16 for 400 eV neon ions. As an alternative in mercury, where the yield curves are straighter, a similar result can be obtained by plotting the normalised yield slope ($\frac{S_1}{\eta}$, where S_1 is the slope and η the energy transfer factor) against atomic number[37].

Stuart and Wehner[43] have made yield measurements at energies close to the threshold by observing the intensity of a spectral line of the sputtered material, excited by spilling electrons in the plasma, using a monochromator and photomultiplier. Yields as low as 10^{-4} atoms per ion could be determined. Measurements were made in mercury vapour using the mercury pool discharge and in argon by freezing the mercury out of the discharge region near the target. The threshold energies were in the range 15 to 45 eV, i.e. lower than those in Wehner's previous experiments, but not as low as in earlier work by other authors, to be described.

TABLE 1 SPUTTERING YIELDS

Target Element	Neon				
	100 eV	200 eV	300 eV	600 eV	
Be	0.012	0.10	0.20	0.56	
*C					
Al	0.031	0.24	0.43	0.83	
Si	0.034	0.13	0.25	0.54	
Ti	0.08	0.22	0.30	0.45	
V	0.06	0.17	0.36	0.55	
Cr	0.18	0.49	0.73	1.05	
Fe	0.18	0.38	0.62	0.97	
Co	0.084	0.41	0.64	0.99	
Ni	0.22	0.46	0.65	1.34	
Cu	0.26	0.84	1.20	2.00	
Ge	0.12	0.32	0.48	0.82	
Zr	0.054	0.17	0.27	0.42	
Nb	0.051	0.16	0.23	0.42	
Mo	0.10	0.24	0.34	0.54	
Ru	0.078	0.26	0.38	0.67	
Rh	0.081	0.36	0.52	0.77	
Pd	0.14	0.59	0.82	1.32	
Ag	0.27	1.00	1.30	1.98	
Hf	0.057	0.15	0.22	0.39	
Ta	0.056	0.13	0.18	0.30	
W	0.038	0.13	0.18	0.32	
Re	0.04	0.15	0.24	0.42	
Os	0.032	0.16	0.24	0.41	
Ir	0.069	0.21	0.30	0.46	
Pt	0.12	0.31	0.44	0.70	
Au	0.20	0.56	0.84	1.18	
Th	0.028	0.11	0.17	0.36	
U	0.063	0.20	0.30	0.52	

The neon and argon yields are
The mercury yields are o

* Extrapolated value
* Graphite

ELDS UNDER NEON, ARGON AND MERCURY ION BOMBARDMENT

	Argon				Mercury			
600 eV	100 eV	200 eV	300 eV	600 eV	100 eV	200 eV	300 eV	400 eV
.56	0.074	0.18	0.29	0.80				
					0.02	0.05	0.09	0.13
.83	0.11	0.35	0.65	1.24		0.14	0.30	
.54	0.07	0.18	0.31	0.53		0.04	0.08	
.45	0.081	0.22	0.33	0.58	0.05	0.14	0.22	0.31
.55	0.11	0.31	0.41	0.70	0.01	0.11	0.21	0.31
.05	0.30	0.67	0.87	1.30	0.02	0.22	0.42	
.97	0.20	0.53	0.76	1.26	0.01	0.13	0.30	0.48
.99	0.15	0.57	0.81	1.36		0.18	0.38	
.34	0.28	0.66	0.95	1.52	0.04	0.25	0.48	0.70
.00	0.48	1.10	1.59	2.30	0.14	0.54	0.94	
.82	0.22	0.50	0.74	1.22		0.21	0.42	0.63
.42	0.12	0.28	0.41	0.75	0.02	0.13	0.24	0.35
.42	0.068	0.25	0.40	0.65		0.09	0.30	0.31
.54	0.13	0.40	0.58	0.93		0.09	0.26	0.43
.67	0.14	0.41	0.68	1.30				
.77	0.19	0.55	0.86	1.46	0.08	0.37	0.66	
.32	0.42	1.00	1.41	2.39	0.13	0.51	0.89	
.98	0.63	1.58	2.20	3.40	0.22	0.85		
.39	0.16	0.35	0.48	0.83		0.17	0.34	0.52
.30	0.10	0.28	0.41	0.62	0.02*	0.18	0.33	
.32	0.068	0.29	0.40	0.62	0.015	0.15	0.35	0.54
.42	0.10	0.37	0.56	0.91		0.26	0.51	
.41	0.057	0.36	0.56	0.95				
.46	0.12	0.43	0.70	1.17	0.07	0.44	0.81	
.70	0.20	0.63	0.95	1.56	0.07	0.52	0.98	
.18	0.32	1.07	1.65	2.43 (500eV)	0.29	0.99		
.36	0.097	0.27	0.42	0.66	0.03	0.23	0.42	0.62
.52	0.14	0.35	0.59	0.97	0.09	0.38	0.67	

elds are from Ref.42.
e obtained from the graphs of Refs.36 and 37.

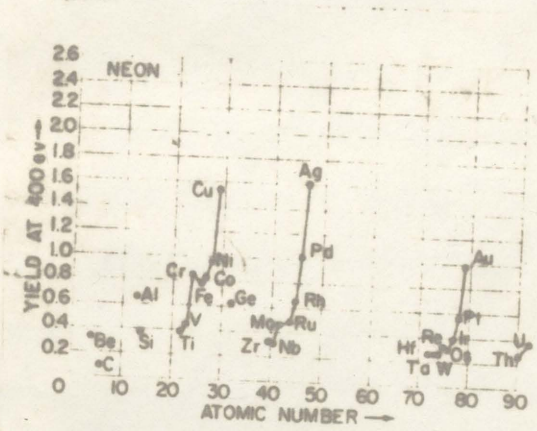

Fig.16. Sputtering yields for 400eV neon ions as a function of the atomic number of the target element.

5.3 Miscellaneous Yield Measurements in Arc Discharges

Morgulis and Tishchenko[44],[45] used radioactive tracer atoms to determine the variation of yield with energy, and the sputtering threshold, the intensity of the γ-radiation from the sputtered deposits being a very sensitive measure of the quantity sputtered. In the original paper[44] yield curves were given for an alloy of nickel and 1% radioactive Co^{60} in argon and mercury vapour and for an electroplated layer of Co^{60} on nickel in mercury vapour. In later experiments[45] a yield curve was obtained for Ir^{192} in argon (Fig.17) and threshold energy values were obtained for the following metals, tagged by the radioactive isotope indicated, in argon and in most cases in helium: Co^{60}, Zn^{65}, Zr^{95}, Ag^{110}, Sb^{124}, Ta^{182}, W^{185}, Ir^{192} and Tl^{204}. The threshold energies are plotted against the heat of sublimation in Fig.18 and are seen to be between 3 and 21 eV, i.e. much lower than those obtained in Wehner's measurements. What is particularly surprising is the low values for helium. The yield curve for Ir^{192} in argon in Fig.17, which is typical of those obtained by Morgulis and Tishchenko, shows not only the usual linear region, in this case above 50eV, but also a second linear region between 25 eV and the threshold energy. In plotting this curve a secondary emission coefficient (not measured) of 0.1 was assumed. The yield at 60 eV agrees approximately with that of Laegreid and Wehner[42]. The yield curves in mercury vapour are probably not reliable due to the presence of a film of mercury on the target. Since measurements were made at very low energies it was necessary to correct the ion energies for the plasma potential by probe

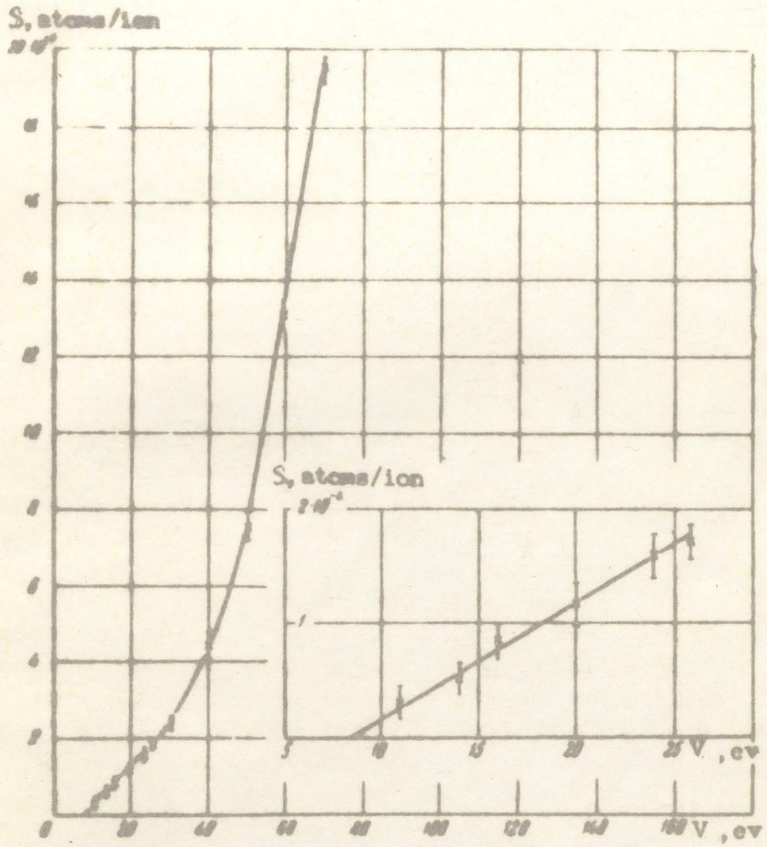

Fig.17. Variation of sputtering yield with ion energy for an Ir^{192} target sputtered by argon ions. Insert: initial section of curve plotted on an enlarged scale.

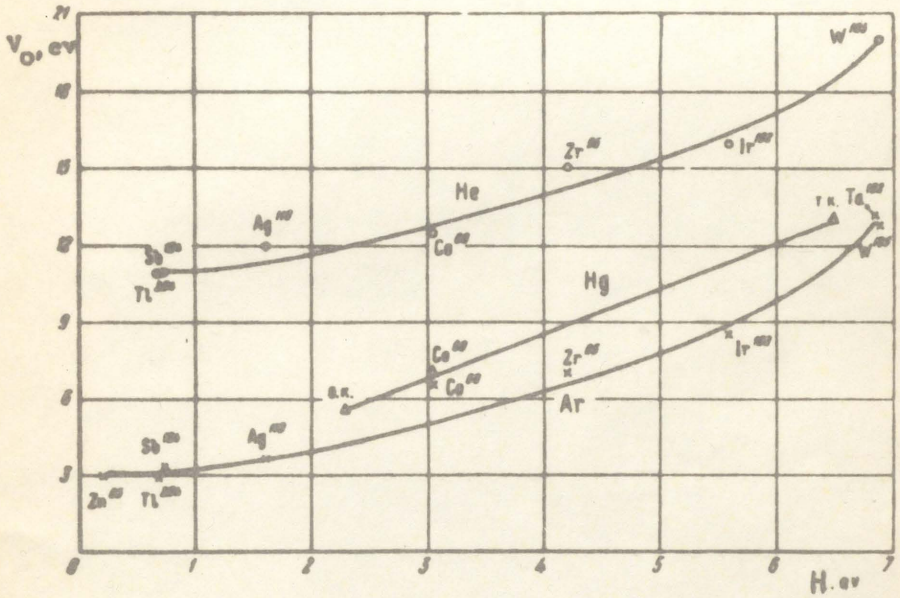

Fig.18. Variation of the threshold energy for sputtering by helium, argon and mercury ions with the heat of sublimation H of the target metal. The points marked T.K. and O.K. are respectively for Th on thoriated cathodes by thermionic emission measurements and Ba on oxide-coated cathodes by contact potential measurements, previously determined.

measurements, as stated in section 4.1. In obtaining the yield curves from the measurements it was assumed that the sputtered particles were emitted with a cosine distribution. As will be seen in section 7.1 this is not strictly true.

Strachan and Harris[46] carried out sputtering measurements on targets of carbon and iron sputtered by mercury and argon ions, by the direct weight loss method, the targets being removed from the discharge tube for the final weighing. The sputtering, uncorrected for secondary emission, varied linearly with energy up to a few kilovolts where the variation changed to proportionality with the square root of the energy, i.e. equation (6) was obeyed with $V_o = 0$. The threshold energies were less than 30 eV, the sputtering approaching zero asymptotically. By observation of the sheath surrounding a spherical target, the actual ion current to the target i_+ (i.e. the total current minus the secondary electron current) was calculated using the Langmuir-Child expression, similar to equation (4), applicable to spherical geometry

$$i_+ = \frac{4}{9}\left(\frac{2e}{m}\right)^{\frac{1}{2}} \frac{V^{3/2}}{\alpha^2} \qquad (4a)$$

where α^2 is a function of (sheath radius)/(target radius) derived mathematically. It was then found that above a few hundred volts energy, the sputtering yield was given by the following relation:

$$S = S_2 . \ln\left(\frac{V}{V_2}\right) \qquad (12)$$

where S_2 and V_2 are constants. However Wehner[36] has cast doubt on the reliability of this method of determining the actual ion current. Measurements were also made for Be, Al, Si, Ni, Cu, Mo, W, Pb and U giving similar results, although no correction was made for secondary emission. The yield was found to increase roughly as (the atomic weight of the target)$^{1.3}$ and was greater for the heavier ion.

Sputtering measurements on single crystals of germanium and silicon in argon were performed by Wolsky[47], using a vacuum microbalance to determine the loss of weight of the target during the sputtering. Although this experiment is included under "arc discharge measurements of yield", the ion currents used, 1 to 12 $\mu A/cm^2$, were more typical of ion beam measurements. As a result, to obtain clean sputtering conditions, ultra high vacuum techniques were necessary, the system being evacuated to 10^{-9} mm Hg before filling with 10^{-3} to 10^{-4} mm Hg of argon.

The sputtering yields (not corrected for secondary emission) were found to vary linearly with energy above 300 eV in silicon and 100 eV in germanium, but a sharp drop in yield occurred below 100 eV in germanium, a threshold energy of 46 eV being obtained. This dependence of yield with energy was not confirmed in the experiments of Laegreid, Wehner and Meckel[41], who obtained a more linear variation at low energies. They suggest that the plasma potential, and hence the bombarding energy of the ions, was rather undetermined in Wolsky's discharge, due to the low ion current density.

Recently Wolsky and Zdanuk[48] have compared the yields for silicon sputtered by singly and doubly charged argon ions, the relative proportions of the two types of ions being varied by means of the main discharge voltage. If sputtering were determined purely by the kinetic energy of the ions, the yield $S_v(A^{++})$ for A^{++} ions accelerated by potential difference V would equal the yield $S_{2v}(A^{+})$ for A^{+} ions accelerated by $2V$. I.e.

$$S_v(A^{++}) = S_{2v}(A^{+})$$

However it was found that at low energies

$$S_v(A^{++}) \simeq 4\, S_{2v}(A^{+})$$

The threshold for A^{+} ions was 15-20eV. It was therefore suggested by Wolsky and Zdanuk that the unusual shape of Wolsky's yield curve in germanium was due to the presence of A^{++} ions from the 275V main discharge.

The yields obtained by Wolsky and Zdanuk[49] for silicon in argon were greater than those of Laegreid et al.[42] above 100eV due, it was suggested, to the high temperature (400-500°C) attained by the latter's targets during bombardment.

Koedam[50] carried out yield measurements on polycrystalline silver and single crystals of copper and nickel in neon, argon and krypton. The targets were immersed in a plasma created by an electron beam, which was prevented from spreading by an axial magnetic field of about 800 gauss. The ion energy range for the silver targets was 50-250eV with an energy spread of about 10eV. The yields were determined from observations of the optical transmission of the sputtered deposits on a glass plate at 5,470 Å and 6,700 Å, in absolute units for silver but only relatively for the single crystals. In the case of the single crystals it was the (110) surface which was bombarded with normally incident ions and the sputtered material was collected normally to the (110) surface. However, with copper the same yields were obtained by bombarding the (111) surface, the sputtered material still being collected normally to the (110) surface. The yield curves were linear over most of the energy range, except for a low energy tail. In the case of polycrystalline silver, however, the yields in neon and argon were lower than those of Laegreid and Wehner[42]. The threshold energy for silver in argon was below 20eV.

Weijsenfeld, Hoogendoorn and Koedam[51] have extended the measurements to copper, nickel, iron and molybdenum in neon, argon krypton and xenon, over the energy range 100 to 1000eV. Fig.19 shows the yield curves obtained. There was good agreement with the results of Laegreid and Wehner[42] for copper and nickel in neon and argon,

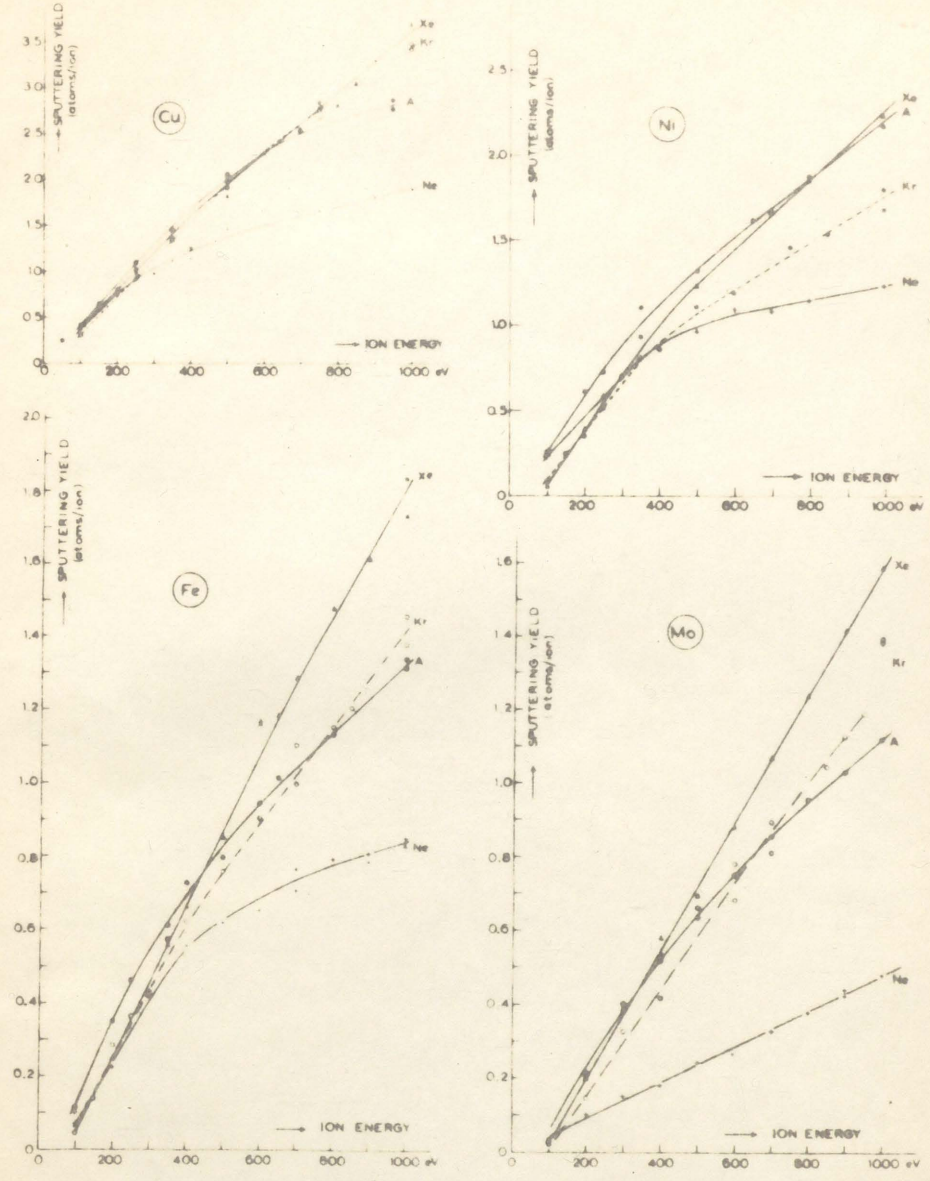

Fig.19. Variation of sputtering yield with ion energy for copper, nickel, iron and molybdenum bombarded by neon, argon, krypton and xenon ions.

except at high energies where the neon values fell below those of Laegreid. In the case of iron and molybdenum the yields were below those of Laegreid and Wehner.

5.4 Yield Measurements With Ion Beams

One of the first attempts to use an ion beam for sputtering yield measurements was made by Timoshenko[52]. An argon ion beam of energy up to 6keV, from a capillary arc, was incident upon a silver target in a chamber evacuated to 5×10^{-5} mm Hg. The sputtering yield was determined from the weight loss of the target, the amount sputtered being large (several milligrams). By applying suitable potentials between the target and the ion focusing cylinder, secondary electrons were returned to the target. Part of the ion current, which was about 200μA, passed to the target holder and the actual sputtering current had to be obtained from the ratio of the area of the target to that of the beam, assuming uniform current density. This was shown to be so by means of concentric diaphragms placed in the ion beam. The variation of yield with energy is shown in Fig.20 and is seen to be unusual, and was not confirmed by the experiments of Keywell described below.

Keywell[53] used an ion beam from a Philips ion gauge discharge to sputter a silver target with argon ions. The target was

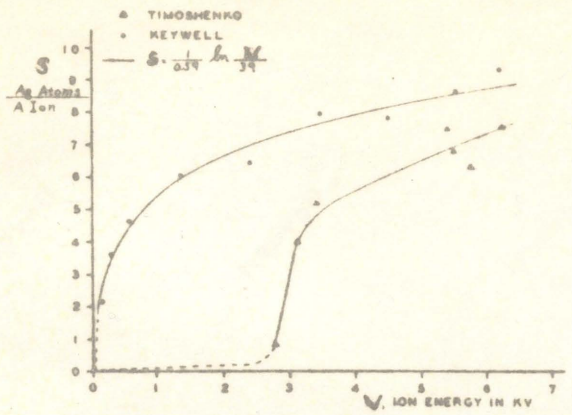

Fig.20. Variation of sputtering yield with ion energy for silver sputtered by argon ions, showing the results of Timoshenko, and of Keywell to which the neutron cooling theory is applied.

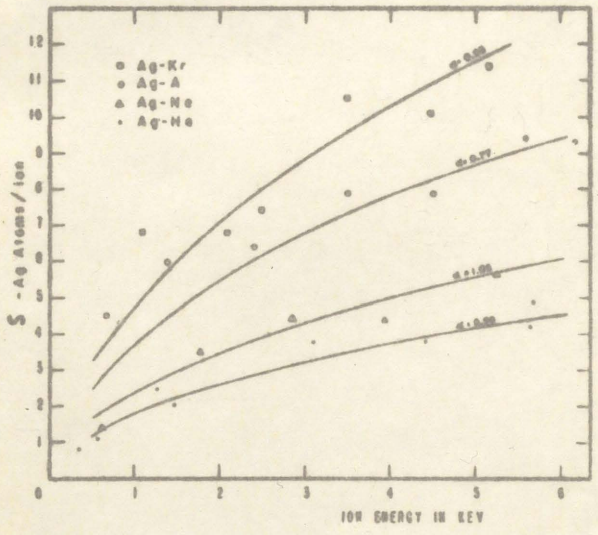

Fig.21. Variation of sputtering yield with ion energy for silver sputtered by helium, neon, argon and krypton, showing the application of Keywell's radiation damage theory.

surrounded by a shield at a more negative potential to return secondary electrons to the target, but the shield was not used for ion energies below 500eV. The ion current density was of the order of 50μA/cm^2 at a gas pressure of 1.2 microns and yield measurements were obtained for energies up to 7keV. The yield was proportional to the logarithm of the ion energy, i.e. equation (12) was obeyed, and Keywell explained this by a sputtering theory based on that of neutron cooling (see section 10.2.1). The yield curve is shown in Fig.20 along with that of Timoshenko.. Wehner[8] has pointed out that the 1,800V Philips ion gauge discharge would have resulted in multiply charged ions being formed, and would have given considerable energy spread to the ion beam.

Keywell[54] later extended his experiments to silver in krypton, neon and helium, copper in krypton and argon, and lead in argon and helium and explained his results by means of a radiation damage theory (section 10.2.1) which was an extension of the neutron cooling theory. Fig.21 shows the theoretical curves drawn through the experimental points for the sputtering of silver, but on comparing this with Fig.20 the fit is seen to be less satisfactory (although applicable to more gas-metal combinations). The magnitude of the sputtering in helium is surprising and suggests the presence of impurities in the gas.

Singly charged ions of helium, neon, argon and xenon were used by Bradley[55] to sputter targets of sodium and potassium,

prepared by vacuum distillation. The ions were of 0 to 1800eV energy with 2 to 4eV energy spread, from a Finkelstein type ion source with a hot cathode and a magnetic field of 200 gauss. The impurity gas pressure under operating conditions did not exceed 5×10^{-8} mm Hg. Secondary electrons from the target were collected by an electrode 40 volts positive to the target. The sputtering yield, in arbitrary units, was determined with a surface ionisation detector, consisting of a hot platinum electrode which caused incident sputtered atoms to be ionised positively and attracted to an electrode at a negative potential. This was a very sensitive method of measuring sputtering, but unfortunately it can only be applied to the alkali metals, since it depends on the ionisation potential for the atoms being less than the work function of the hot electrode. A small current to the ion collector, when the platinum electrode was cold, was ascribed to ions reflected from the target. At 1000eV this current was 50% of the true current in helium and 5% in xenon. The ion current density to the target was only of the order of $1\mu A/cm^2$ and hence the formation of surface impurity layers may have occurred during the sputtering.

Sputtering of sodium by neon ions was detected at 5 volts energy, by helium and argon at 10 volts and by xenon at 30 volts. The sputtering yields for helium and neon ions varied linearly with the logarithm of the energy (equation (12)), as in Keywell's experiments, but for argon and xenon the yield was more linear with the square root

of the energy, or the momentum of the ion (equation (6)). At low momenta the yields were nearly the same for all ions, at the same momentum relative to the centre of mass of the ion and its target atom. This suggests that the yield is determined primarily by the momentum, and hence kinetic energy, transferred to a single target atom in a single two-body collision. At high energies the yields were in the order of increasing ionic mass.

A number of workers have made yield measurements at high energies using electromagnetic isotope separators as ion sources, the yields being determined in most cases from the weight loss of the target mounted in a Faraday cage, arranged so that automatic compensation occurs for the secondary electron emission. In particular mention must be made of the work of Yonts, Normand and Harrison[56]; Grønlund and Moore[57]; Rol, Fluit and Kistemaker[58]; and Almén and Bruce[59].

Yonts et al.[56], using copper targets, found that whereas for argon ions the yield increased with energy between 5 and 27.5keV, with deuterium the yield decreased between 10 and 40keV, and with helium between 15 and 40keV. However the reliability of the measurements is reduced by the observation of a pressure dependance of the yield, which would not be expected at the pressures used (about 10^{-4} mm Hg, see section 6.2). It was explained as due to the formation of surface impurity layers and was considered further in a later paper[60].

Grønlund and Moore[57] sputtered silver containing the radio-active isotope Ag^{110} with H^+, D^+, H_2^+, D_2^+, D_3^+, He^+, N^+, O^+ and Ne^+ ions, over the energy range 2 to 12keV. Broad maxima in the yield curves were observed at 4 to 6keV.

Rol et al.[58] obtained yield curves for copper targets sputtered by the following ions of 5 to 25keV energy: N^+, Ne^+, Na^+, Si^+, P^+, S^+, Cl^+, A^+, K^+, Cu^+, Zn^+, Cd^+, I^+, Hg^+ and Tl^+. The yields increased with ionic mass, and the increase in yield with energy was greater for the heavier elements than for the lighter. In the latter case the yields passed through a maximum or tended to a constant value at high energies. The argon curve could be extrapolated through the results of Keywell[54], but were somewhat lower and showed less energy dependance than the less reliable curve of Yonts et al[56]. The mercury curve showed abnormally large energy dependance, probably due to contamination of the copper with mercury, and did not agree with the results of Wehner and Rosenberg[61] to be described.

Almén and Bruce[59] obtained yield curves for Cu, Ag, Mo, Pa and Sn sputtered by Ne^+, A^+, Kr^+ and Xe^+ and in some cases N^+ ions, at energies up to 65keV. Where comparison is possible very good agreement was obtained with the results of Keywell[54] and Rol et al[58]. Yields for 45keV krypton ions incident on 28 different target elements are shown in Fig.22, indicating the variation within the periods of the periodic table, in a similar fashion to Fig.16 for 400eV neon ions

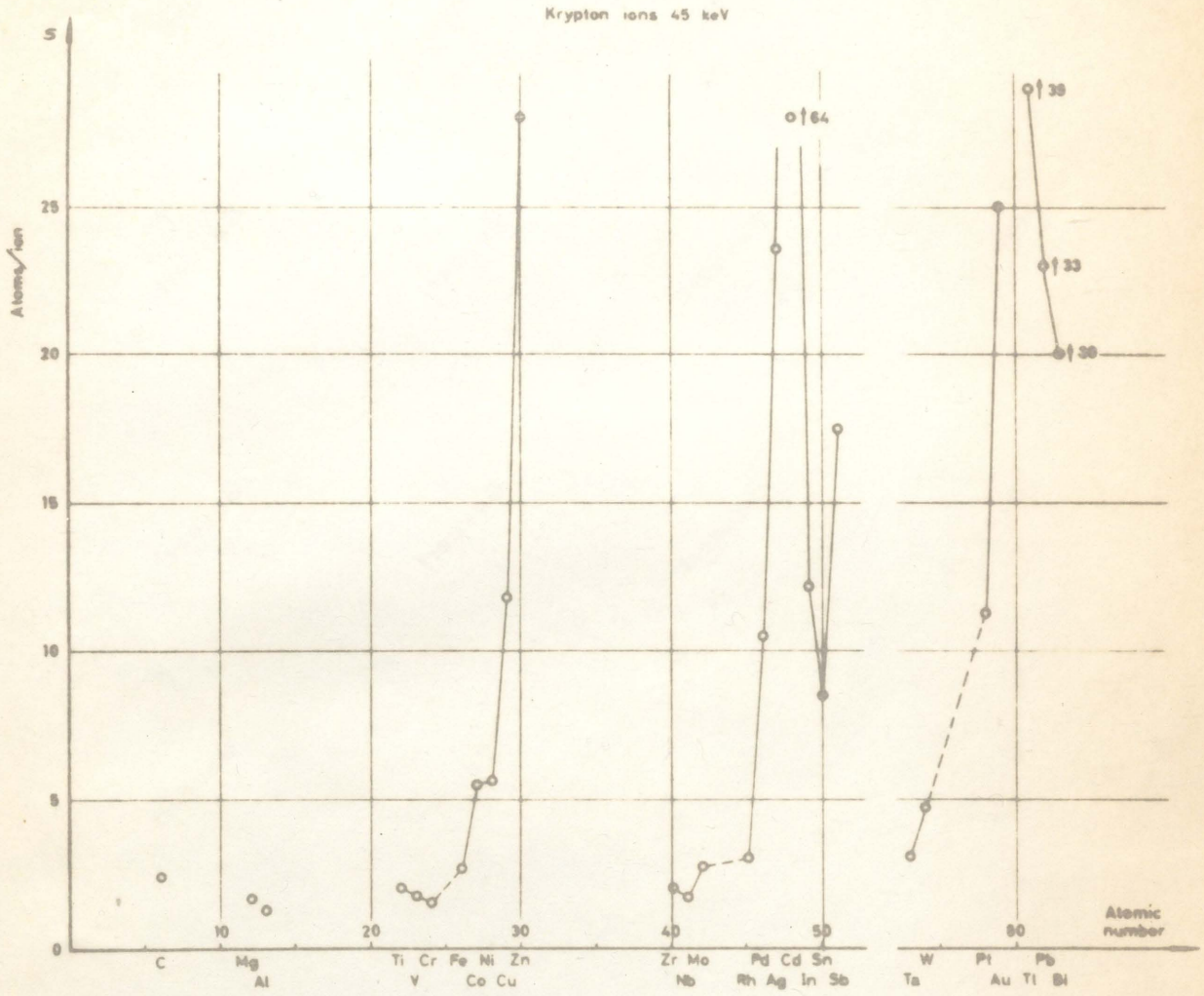

Fig.22. Sputtering yields for 45keV krypton ions bombarding different target materials, as a function of the atomic number of the target element.

as observed by Laegreid and Wehner[42]. Fig.23 shows the variation of yield for copper, silver, and tantalum targets, sputtered by 68 different ions of 45keV. A similar diagram was also given for the sputtering of various targets by ions of the same element.

Wehner and Rosenberg[61] have obtained yield curves for fourteen metals of the fourth, fifth and sixth periods, sputtered by a mercury ion beam of 4 to 15keV from a modified version of the demountable mercury pool cathode tube used in Wehner's lower energy arc discharge measurements. The sputtering yields were calculated from the time required for the ion beam to penetrate the target in the form of a thin foil of known thickness (0.025 mm). An ion collector plate behind the foil, at the same potential, collected ions penetrating the foil, and the time integral of this current was subtracted from the measured ion current. After a series of holes had been sputtered, the foil was removed and the areas of the holes measured with a shadowgraph at 20x magnification. The yield curves were of a similar form to those of other ion beam measurements, although no maxima were observed. Unfortunately no measurements were made below 4keV and hence it is difficult to compare the results with Wehner's arc discharge measurements, the upper energy of which did not normally exceed 400eV. No correction was made for secondary emission as measurements of the current-voltage characteristic, when small voltages were applied between the foil and ion collector plate, indicated that γ was less than 8%.

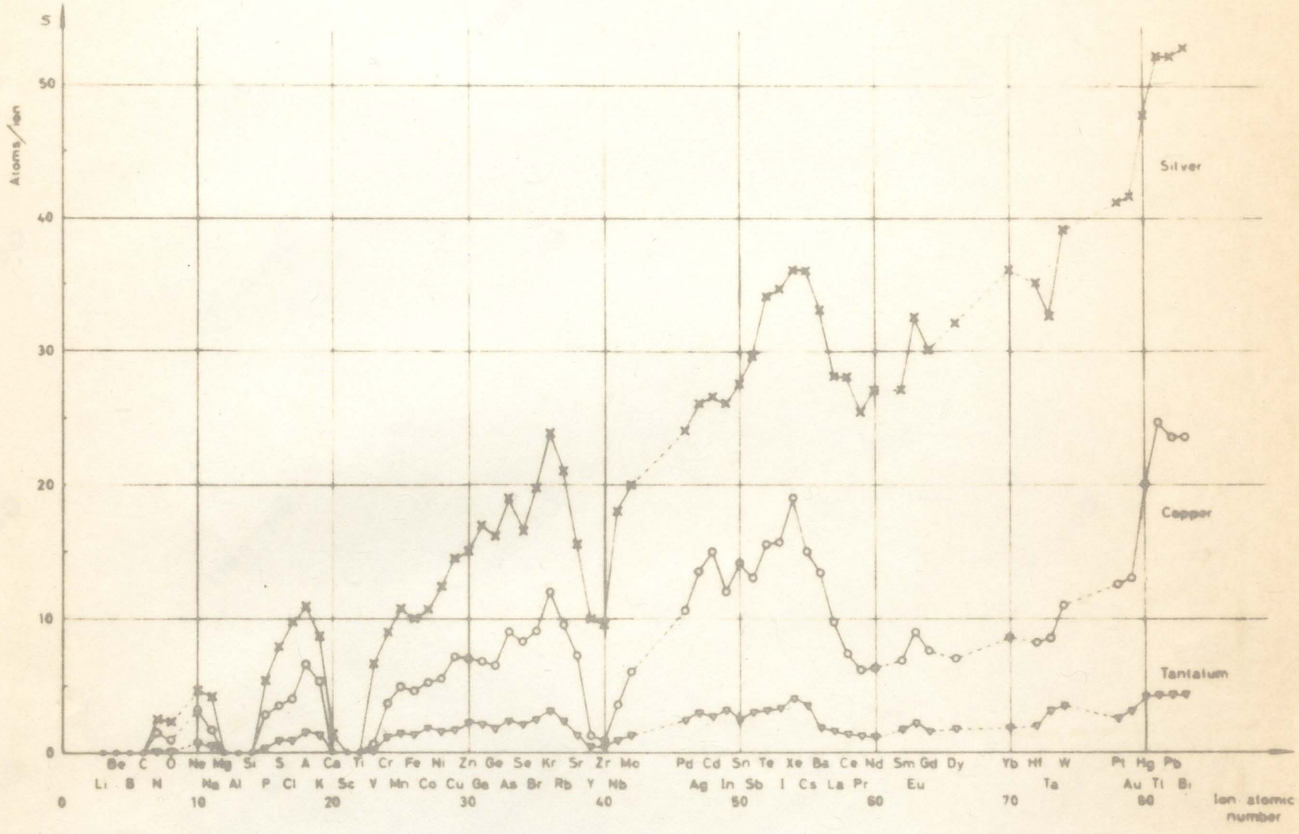

Fig.23. Sputtering yields for copper, silver and tantalum bombarded 45 keV ions of different elements, as a function of the atomic number of the element.

Recently, measurements have been made of the yield for vitreous silica bombarded by 20 to 60keV xenon ions, by Hines and Wallor[62]. This is probably the only experiment on the sputtering of insulators which warrants consideration. The targets were ground and polished before bombardment. The ion beam, which was magnetically analyzed, was incident normally on the target and had a current density of $500\mu A/cm^2$ in a vacuum of 10^{-5} mm Hg. The current was measured by placing a Faraday cup connected to a galvanometer, in the ion beam. The charge deposited on the insulating target was neutralized by electrons from a hot tungsten filament. The amount of material sputtered was measured by observation of the reflection interference fringes under vertically incident sodium light (589mμ) between the sputtered surface and an optically flat reference plate. The area of each light and dark fringe was measured with a planimeter and the volume of the sputtered cavity calculated with Simpson's rule. The yield values obtained were at 20keV, 0.71; 30keV, 0.85; 40keV, 1.78; 50keV, 1.74; 60keV, 1.31. It will be noticed that as with many metal targets at high energies, a maximum in yield was obtained.

Finally mention must be made of a new method for measuring sputtering, developed by McKeown[63]. An argon ion beam, from a Finkelstein ion source, bombarded a gold plated layer on a 10 Mc/s quartz crystal connected to an oscillator. The sputtering of the gold was observed as a change in frequency of the oscillator. Although McKeown was working in the energy region below 100eV, with a background

gas pressure of 10^{-4} mm Hg and a beam current density of $3\mu A/cm^2$ the yield curve obtained agreed with that of Wehner over the energy range 50 to 100eV, but the threshold was about 10eV. The yield values were not corrected for secondary emission. The reason for the good agreement was the presence of a 0 to 270eV neutral beam in the ion beam, which did not vary with the ion beam. This neutral beam kept the target clean, even at low energies. The sputtering due to the neutral beam was subtracted from the total to obtain the yield curve. In the absence of the neutral beam the sputtering threshold was about 60eV. No information is available on the yield for the neutral beam as the intensity and energy distribution are not given, only the energy limits (0-270eV) being quoted.

This method of measuring sputtering can be used for all target materials, it gives the yield absolutely ~~(except for the secondary emission correction)~~ and continuously and it can be used when the amount sputtered is extremely small. It is therefore capable of much more universal application than the more usual methods previously described. It is to be hoped, however, that in future more attention will be given to obtaining clean conditions, without the need for a neutral beam.

5.5 Summary of the Results on the Variation of Yield with Ion Energy

The experiments described in the previous sections have produced the following equations for the yield S (or $\frac{S}{1+\gamma}$) as a function

of ion energy V or velocity v

$$S = S_0 (V - V_0)^2 \qquad (7)$$

$$S = S_1 (V - V_1) \qquad (9)$$

$$S = S_2 \ln \left(\frac{V}{V_2} \right) \qquad (12)$$

$$S = A(v - v_0) = S_3 \left(\sqrt{V} - \sqrt{V_3} \right) \qquad (6)$$

The most useful equation is (9) which can frequently be applied over an energy range in the several hundred eV region. At higher energies, up to several keV, the results can better be expressed by equations (6) or (12). At higher energies still the yield tends to a saturation value as the energy is increased, or exhibits a maximum as the ions tend to penetrate further into the target. The maximum seems to occur at lower energies as the ionic mass is decreased. At energies below the range covered by equation (9)the yield tends assymptotically to zero as the energy decreases, and can sometimes be expressed by equation (7) over a limited region. However Morgulis and Tishchenko[44],[45] observed a second nearly linear region at yields below 10^{-3}, which would not be detectable in the other experiments described.

Although the constant V_0 (or V_1 of a lower energy linear region) can be considered as a threshold energy, there is probably no

definite threshold as there are always some loosely bound atoms on the surface which can be sputtered by very low energy ions. Hence the more sensitive the detector of sputtering, the lower the threshold appears to be. The constant V_i (for the higher energy linear region if the yield curve is two straight lines) is known as the "cut-in" energy[36]. The lower energy limit to the range over which equation (9) can be applied has been called the "ankle" energy[64].

The most reliable yield measurements in the energy range of most interest in gas discharges, are probably those of Wehner et al. (Table 1) or Weijsenfeld et al. (Fig.19). The early threshold energies obtained by Wehner are definitely much too high, being more identifiable with the energies V_o or V_i, much lower threshold values having been obtained by Morgulis and Tishchenko (Fig.18).

The variation of yield with the atomic number of the target metal is shown in Fig.16 for 400eV neons ions and Fig.22 for 45keV krypton ions, where it can be seen that the yield varies in a similar fashion in the different periods of the periodic table. The variation of yield with atomic number of the bombarding ion at 45keV is shown in Fig.23 for 68 different ions. At the lower energies typical of measurements in arc discharges the choice of suitable ions is much smaller. For the usual gases and vapours used in discharges, the yield seems in general to increase with atomic number, being particularly

small for helium, but as can be seen from Fig.19 for the inert gases, the order of the gases for increasing yield varies with the ion energy.

6. THE EFFECT OF MISCELLANEOUS PARAMETERS ON THE SPUTTERING YIELD

6.1 Current Density

The determinations of yield described in previous sections assume the yield to be independent of the current density. This is found to be so for normally incident ions, provided the current density is high enough to prevent the formation of surface impurity layers. Fig.24 shows the variation of yield with current density, observed by Wehner[35] for platinum bombarded with mercury ions of 100 and 200eV energy at 300 and 650°C. At 650°C and 200eV the yield is independent of current density above $1mA/cm^2$. At 300°C and 200eV, however, the yield only reaches the constant value at $3mA/cm^2$, due to the presence of an impurity layer, probably a mercury film, on the surface. It must be emphasized that the independence of the yield with current density in any sputtering experiment is a valuable check on the purity of the discharge conditions.

6.2 Gas Pressure

At low pressures the yield is independent of pressure, but at high pressures it decreases approximately linearly with increasing pressure, as required by equation (2) for the glow discharge. Similar variations occur if the tube dimensions are varied. This is shown in Fig.25 which was prepared by Penning and Moubis[29] and combines only early arc and glow discharge measurements. The decrease in yield

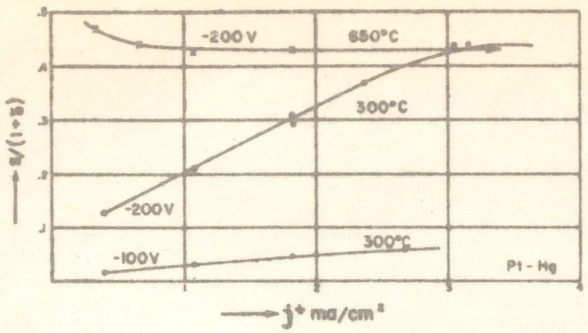

Fig.24. Variation of sputtering yield with ion current density j^+, for platinum bombarded with mercury ions, at different temperatures and ion energies.

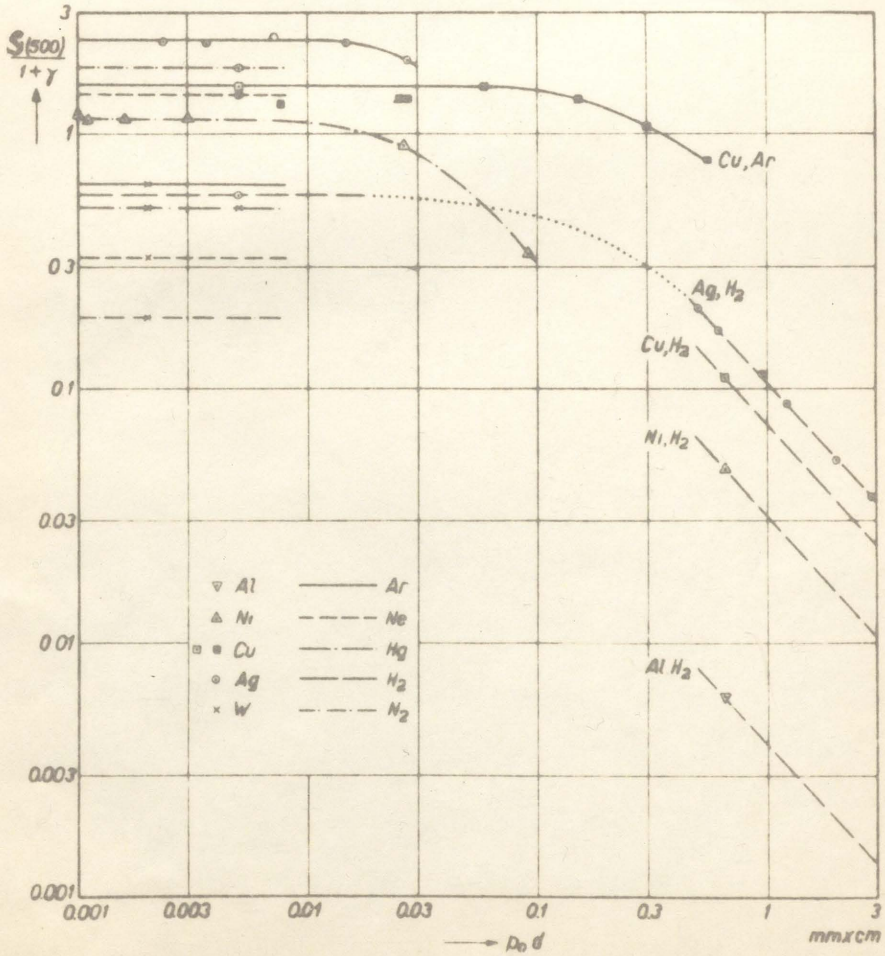

Fig.25. Variation of sputtering yield at 500 eV energy with the product of pressure and electrode separation $p_0 d$

commences at higher pressures than would be expected if the effect were due only to collisions of the ions and sputtered atoms with gas atoms. For example, Penning and Moubis found that for copper in argon the yield had decreased by a factor of a half, from the constant low-pressure value, when the pressure was increased from 20 to 200 microns, although the decrease would have been expected at a pressure 45 times lower! The probable explanation is that at higher pressures there is an increasing probability of oblique incidence of the ions on the target, with a resulting increased yield (See section 6.3). This may compensate for the expected decrease due to ions arriving with lower energy after collision, and back-diffusion of sputtered material to the target. Imperfect compensation may account for the maximum in the yield versus pressure curves of Penning and Moubis referred to in section 3, which can be seen for the solid square points on the copper-argon curve in Fig.25.

If an attempt is made to calculate the yield at low pressures from measurements at high pressures, assuming the sputtered material travels through the gas by diffusion, the yield obtained is much greater than that obtained by direct measurement. For instance, Guentherschulze[10], from observations on silver sputtered in a hydrogen glow discharge at 2 mm Hg and 550 volts cathode fall, obtained a yield of 9.6 atoms per ion. However Guentherschulze and Meyer[32] measured a yield of 0.6 at low pressure for 600eV ion energy. The discrepancy must again be the oblique incidence of the ions.

As mentioned in section 5.4, an apparent variation of yield with pressure was observed by Yonts et al.[56],[60], between 0.04 and 0.08 microns, for copper sputtered by 30keV argon ions in an electromagnetic isotope separator. Since the mean free paths of the ions and sputtered atoms were greater than the dimensions of the apparatus, this was explained as due to the competing effects of contamination of the target by background gases and the cleaning of the target by the ion beam.

6.3 Angle of Incidence

Fetz[65] sputtered molybdenum wires in a mercury pool discharge at 1.5 microns pressure and showed that the yield decreased as the diameter of the wire increased, approaching the value for a plane target. By heating the wires electrically he showed that only part of the effect was due to the different temperatures reached by the wires. The explanation given was the increasing probability for oblique incidence of the ions as the wires were made finer. Whereas a large plane target is bombarded essentially normally, because the initial velocity of the ions on entering the sheath is small compared with that gained in falling through the sheath, with a fine wire target the ions spiral round with constant angular momentum so that they arrive with a tangential component of velocity v_t, related to their tangential velocity at the sheath v_c, by the equation

$$v_t r_t = v_c r_c$$

where r_t and r_c are the radii of the target and sheath respectively. Since for a fine wire $r_t \ll r_c$ the tangential velocity component of the ion on hitting the target can be large and increases as the wire becomes finer. As expected, all the yield results lay on one curve when plotted against $\frac{r_t}{r_c}$, whether $\frac{r_t}{r_c}$ was varied by means of the wire diameter or the plasma density.

Wehner[35],[66] sputtered a polycrystalline metal strip in a low pressure mercury pool discharge and collected the sputtered material on a surrounding cylindrical glass collector. The sputtering was greatest, not on the actual edge of the metal strip, but from a region near the edge, due to the heavy ions not being able to follow the field lines very well and being focused somewhat away from the edge. By protecting one target edge with aquadag to prevent sputtering and observing the effect on the sputtered deposits on the glass, it was shown that the difference in the angle of incidence between the edge and the flat portion of the target had a marked influence on the sputtering. At low ion energies the sputtering was much greater from the edge regions under oblique incidence than from the larger normally bombarded middle portion of the target, but at higher energies the difference was less pronounced. It was concluded that the threshold energy for oblique incidence was markedly less than for normal incidence of the ions.

More direct information on the effect of the angle of incidence on sputtering yields has been obtained by Wehner[67]. Ion

beams were extracted from a low pressure (0.2 micron) mercury plasma through small holes in a graphite plate, negative with respect to the plasma. With hole diameters small compared to the ion sheath thickness, approximately parallel beams entered the field and plasma free region behind the plate, and could be checked for beam width and uniformity by observing the sputtering of a silver disc behind one of the plate holes. Small polycrystalline metal spheres, with diameters less than the beam diameter, were mounted opposite the holes in the graphite plate, but were connected electrically to the plate. The spheres were sputtered by the mercury ion beams and the angle effect studied by measuring the thickness of material removed in different zones using shadow micrographs of the spheres. Absolute yields for normal incidence were obtained by the weight-loss method. The ion energy range was 125 to 800eV, with a beam current density of $1mA/cm^2$ at 150eV. The metals studied could be divided into three groups: (1) gold, silver, copper and platinum, which showed only a slight variation with angle but fairly high yields at normal incidence; (2) nickel and tungsten with a moderate angle effect; and (3) iron, tantalum and molybdenum with a very pronounced effect. In most cases the yield showed a maximum for an angle of incidence of 50 to 60° from the normal. Fig.26 shows the results obtained for tungsten. It will be noticed that the angles are measured from the tangent to the surface, not the normal.

Rol, Fluit and Kistemaker[58] observed copper sputtered by argon and thalium ions from an electromagnetic isotope separator, at the

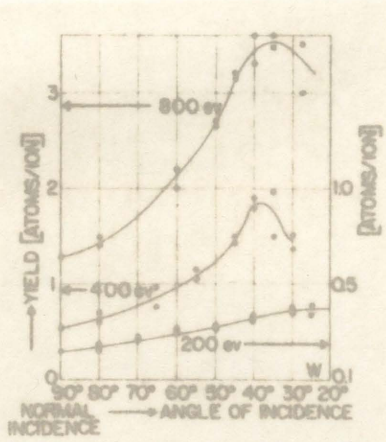

Fig.26. Sputtering yield of tungsten as a function of the angle of incidence of mercury ions, at three different ion energies.

much higher energy of 20keV. The angle of incidence was only varied from 0 to 50° to the normal and was not well defined due to convergence of the ion beam. The yield S_ϕ varied with the angle of incidence ϕ according to the relation

$$S_\phi = S_o \frac{2-\cos\phi}{\cos\phi} \qquad \text{for } \phi < 45°$$

where S_o is the yield for normal incidence.

The copper-argon combination has also been studied by Molchanov and Tel'kovskii[68] at 27keV. The angle of incidence of the ion beam could be varied from 0 to 84°, the error in the angle not exceeding ±1° at 84°. The yield was determined from the loss of weight of the target. The yield was inversely proportional to the cosine of the angle of incidence up to 70°; maximum yield was observed at about 80°; after which it decreased when fast reflected particles were observed.

Almén and Bruce[59] have shown that for copper, nickel and tantalum sputtered by 45keV krypton or neon ions the yield varies according to the relation $S_\phi = \frac{S_o}{\cos^{3/2}\phi}$ up to an angle of incidence of 60°, but that the relation does not apply to silver targets.

The measurements so far described have all been carried out on polycrystalline targets. In the case of single crystals the effects

are more complicated. Rol et al.[69] bombarded the (100) plane of a copper monocrystal with 20keV argon ions and observed a yield maximum at an angle of incidence of 24° and minima at 3° and 38°. The measurements did not extend beyond 50°. Similar measurements have been made by Molchanov et al.[70] for 27keV argon ions on the (100) plane of copper and nickel. Minimum yield occurred at 0°, 35 ± 1° and 55 ± 1°, i.e. in the [100], [111] and [112] directions. Recently Almén and Bruce[59] bombarded the (111) plane of copper with 45keV krypton ions and obtained similar results.

6.4 Target Temperature

Early experiments, for instance that of the General Electric Company[30], suggested that the target temperature had little influence on the sputtering yield. However, Fetz[65] found the yield from a molybdenum target bombarded by mercury ions practically doubled when the target temperature was raised from 400° to 1000°C. The explanation may be contamination of the target since Wehner[35] found temperature effects at low current densities, but not at high, for platinum sputtered by mercury ions (see section 6.1 and Fig.24). As mentioned in section 5.3, the discrepancy between the yields for silicon in argon between Laegreid et al.[42] and Wolsky and Zdanuk[49] has been explained by the latter as being due to the higher temperature of the target in the experiments of Laegreid et al.

It must be concluded that information on the influence of temperature is very limited, most authors ignoring the possibility of any temperature effect in their experiments.

7. THE ANGULAR DISTRIBUTION OF SPUTTERED MATERIAL

7.1 Polycrystalline Targets

The earliest attempt to determine the angular distribution of sputtered atoms was made by Seeliger and Sommermeyer[71]. A beam of canal rays, of energies from 5 to 10keV, from an argon discharge, entered a mica cylinder and was incident on a strip of silver or molten gallium along the cylinder wall. The mica cylinder became covered with a uniform deposit of sputtered material, indicating a cosine distribution law, for any angle of incidence of the ion beam.

The cosine distribution of sputtered material for silver bombarded normally by high energy ions has been confirmed by O'Briain, Lindner and Moore[72] using beams of 9250eV H^+, H_2^+ and D^+ ions. The silver target contained Ag^{110} as tracer so that the distribution of sputtered silver over the collector could be determined by its radioactivity. The measurements were later extended by Grønlund and Moore[57], to D^+ and Ne^+ ions incident on silver at 60° to the normal. There was general agreement with the cosine law, except for some additional sputtering in the forward direction, for D^+ ions.

Cobić and Perović[73] determined the angular distribution for copper and lead targets bombarded with 17keV A^+, Kr^+ and Xe^+ ions. They found deviations from the cosine law, particularly if the targets

were cooled with water or liquid air, the distributions being "over-cosine"; i.e. more material was emitted normally than for a cosine law. Rol, Fluit and Kistemaker[58] measured the angular distribution for copper sputtered by argon ions of 20keV. They found the distribution was Gaussian ("over-cosine") rather than cosine and was symmetrical, even for obliquely incident ions.

At low ion energies, Wehner[66] had previously obtained evidence that obliquely incident ions caused preferential sputtering in the forward direction. Recently, Wehner and Rosenberg[74] have measured the angular distributions for several metals bombarded by normally or obliquely incident ions of 100 to 1000eV energy in a mercury pool discharge. A ribbon, placed round the inside of the cylinder surrounding the central target, collected the sputtered material and the thickness of the deposit on the ribbon was determined photometrically. The angular distribution for normal bombardment was "under-cosine" but tended towards cosine as the energy was increased. Molybdenum and iron had a much greater tendency than nickel, platinum or germanium to be sputtered to the sides under normal bombardment, particularly at low energies. Fig.27(a) is a polar diagram of the distribution for molybdenum. Fig.27(b) shows the distribution for molybdenum under oblique bombardment. Nickel showed less tendency than molybdenum to eject material in the forward direction.

Stein and Hurlbut[75] have measured the angular distribution of potassium atoms sputtered by beams of He^+, Ne^+, A^+, Kr^+ and Xe^+ ions

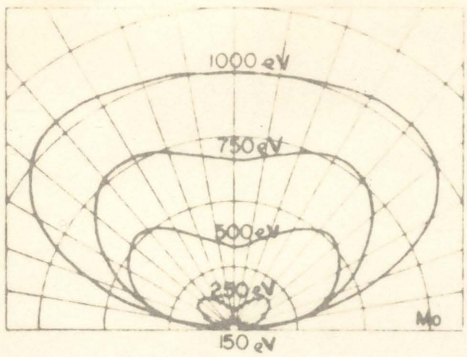

(a)

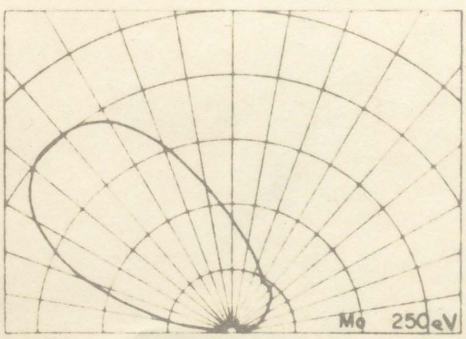

(b)

Fig.27. Polar diagrams of material sputtered from molybdenum targets by mercury ions of various energies: (a) normal incidence, (b) oblique incidence.

of 50 to 240eV energy and various angles of incidence. The sputtered atoms were detected by a surface ionization detector similar to that of Bradley[55] (section 5.4). The sputtered atoms again tended to be ejected in the forward direction, especially at the lower energies, but the distribution became more nearly cosine at the higher energies.

7.2 Monocrystalline Targets

The distribution of sputtered material from single crystal targets was first observed by Wehner[76]. The targets were sputtered by low energy (50-150eV) mercury ions in a mercury pool discharge at 1 micron pressure, the sputtered material being deposited on a glass collector plate. The deposits were in the form of simple patterns characteristic of the crystal structure and the plane being bombarded. In the case of silver or copper, which have face centred cubic (f.c.c.) structures, bombarding the (111) plane gave a deposit of three rather diffuse patches in a symmetrical pattern, the (100) plane four symmetrical patches, and the (110) plane a central deposit surrounded by four patches in two-fold symmetry. In every case the patches corresponded to emission in the $\langle 110 \rangle$ directions — the close-packed direction for a f.c.c. structure. For W, Mo and α-Fe, the emission was in the $\langle 111 \rangle$ directions which are again the close-packed directions (b.c.c. structure). For germanium (diamond structure) the ejection was again in the $\langle 111 \rangle$ close-packed directions. The deposit patterns

were not affected by the development of etch patterns on the target surface.

In the case of silver, Wehner[35] observed the deposit pattern at three different energies: 50, 100 and 150eV. The largest variation in pattern with energy occurred for the (110) plane, the centre spot tending to disappear at very low energies; sputtering in the [110] direction normal to the surface requires a 180° change of the direction of the original momentum, while the four other ⟨110⟩ directions require less and hence predominate near threshold. In addition, at very low energies only atoms with a close-packed direction not obstructed by neighbour atoms can be sputtered, whereas at higher energies atoms can escape from positions where neighbour atoms interfere with the close-packed directions. The obstructing atoms deflect those sputtered and cause changes in the deposit patterns.

The observations were later extended by Anderson and Wehner[77] and the deposit patterns examined in more detail. At higher energies bombarding the (111) surfaces of Au, Cu and Ni gave six deposits instead of three, due, it was suggested, to disorientation of the surface layers. The "damage" could be annealed out by operating at higher target temperatures. In some cases deposits corresponding to next-nearest neighbours were observed. With germanium the patterns were similar to those for b.c.c. crystals, due presumably to the formation of interstitials near the surface.

Similar results have been obtained by Koedam[50] for copper sputtered by neon, argon and krypton ions. Bombardment of the (100) surface gave the four $\langle 110 \rangle$ deposits, and at high energies a deposit along the $[100]$ surface normal, this deposit being the most important above 2keV. The (110) surface showed a pattern of five $\langle 110 \rangle$ deposits (one along the surface normal) and suggested the presence of two $\langle 100 \rangle$ deposits. The (111) surface gave the six deposits observed by Anderson and Wehner[77], three in the $\langle 110 \rangle$ directions and three roughly in the $\langle 114 \rangle$ directions due, it was suggested, to stacking faults caused by the ion bombardment. Similar results were obtained for nickel but germanium gave only a vague deposit pattern. The subject of deposit patterns from monocrystalline targets was considered by Koedam in considerable detail in his thesis[50].

Deposit patterns can still be observed at much higher energies. Rol et al[69] observed the patterns produced by 20keV argon ions incident on the (111) and (100) surfaces of copper and obtained similar patterns to those at lower energies. Yurasova et al[78] used argon and hydrogen ions with energies up to 50keV incident normally and obliquely on the (100) surface of copper, and observed deposits in the four $\langle 110 \rangle$ directions, the $[100]$ normal and also four directions near the $\langle 113 \rangle$ and $\langle 112 \rangle$ directions. The density distribution of material in the $\langle 110 \rangle$ and $[100]$ deposits was found to obey the cosine law.

7.3 Etch Effects Due to Sputtering

Closely related to the angular distribution of sputtered material is the etching of the target. Wehner[35] has shown, if a polycrystalline material is bombarded by low energy ions, crystallites with different orientation are attacked at different rates. Grain boundaries are generally sputtered at a higher rate and appear as furrows. Oriented pits or hillocks are often observed, characteristic of the grain orientation. In fact the appearance of the surface frequently resembles that due to certain chemical etchants.

The effect of bombarding single crystals was also observed. The (111) surface of a silver single-crystal rod, sputtered with 150eV mercury ions, tended to develop {110} facets. It was suggested that this was due to crystal growth rather than etching. To show that this was possible, a tungsten single-crystal wire was arranged on the axis of a polycrystalline tungsten cylinder, the wire being at -70V and the cylinder at -400V relative to the plasma produced by a mercury pool discharge. Under these conditions tungsten atoms were deposited on the wire at a higher rate than they were sputtered off, and the wire grew as a single crystal from 0.3mm to 0.7mm diameter in 40 hours. If the wire was not under ion bombardment, however, the tungsten atoms were not deposited in single crystal form, the ion bombardment being required to keep the surface free of impurities.

The etch effects due to obliquely incident ion beams have been observed by a number of workers. For example, Magnuson et al.[79] bombarded polycrystalline Cu, Au, Al, W, Ta, Mo and Ni, and single crystals of Cu, with 500eV mercury ions and observed patterns of hillocks oriented parallel to the direction of the ion beam, and in the case of Cu and Ni steps perpendicular to the beam.

8. THE NATURE OF THE SPUTTERED PARTICLES

Information obtained in the glow discharge, referred to in section 2.3, had suggested that sputtered material was mainly in the form of uncharged atoms. Information on this has now been obtained by Honig[80], using an ion beam of energy 30 to 400eV and of current density up to 30μA/cm^2 at 100eV. The ions used were Ne^+, A^+, Kr^+ and Xe^+ and the targets polycrystalline silver and the (111) plane of monocrystalline n-type germanium. Sputtered particles were identified by means of a 180° mass spectrometer, neutrals being ionized by a 100μA electron beam which was turned off for observations on ions.

With the silver target, Ag^+, Ag_2^+, Ag_3^+, Ag_2O^-, Ag_2^- and $Ag_2O_2^-$ sputtered ions were observed, in order of decreasing intensity, reflected bombarding ions, and a very long list of impurities, but neutral Ag was not detected due to the experimental conditions at the time. However, sputtering of the germanium target suggested that neutrals were about one hundred times more abundant than ions, although only about 10^{-4} of the neutrals could be ionized by the electron beam. The particles identified were Ge, Ge_2, Ge^+, Ge_2^+, GeH^+, $GeOH^+$. Ge_2O^+, and various impurity molecules and ions. The intensity ratio of Ge_2^+ to Ge^+ was 1 to 50 for 400eV A^+ ions.

Although this work is interesting it was carried out under rather impure conditions. The background gas pressure was about 10^{-7} mm Hg, which would require a higher bombarding current density to keep the target clean.

Similar observations have been made by a number of workers on the ionic component only of the sputtered particles ("secondary [redacted] ion emission"). Mention must be made of the work of Bradley[81] who bombarded Mo, Ta and Pt with inert gas ions of 0 to 1keV energy under cleaner conditions than the above, and Stanton[82] using Be and other targets and inert gas ions of 0 to 3keV.

8.1 The Velocities of Sputtered Atoms

Glow discharge observations of Baum,[20] referred to in section 2.3, had suggested that sputtered atoms were emitted with velocities of the order of those of evaporated atoms. However, the observations of Guentherschulze[12] suggested that sputtered atoms have much higher energies than evaporated atoms.

Retarding potential measurements on secondary positive ions have been used to determine their velocities. Honig[80] found the most probable emission energy for Ge^+ ions sputtered by Kr^+ ions of 100 to 400eV energy was about 2eV, a few ions having energies up to about 20eV. Stanton[82] for Be^+ ions sputtered by 1000eV Ne^+ ions, could detect ions with energies up to 300eV, although a large fraction of the ions had energies below 10eV.

Recently Wehner[83],[84] has measured the emission velocities of sputtered atoms by two different methods. In the first method[83]

atoms sputtered from a target in a mercury pool discharge plasma were deposited on the underside of a quartz pan suspended from a quartz helix. If the mass deposited per second was m and the average velocity component normal to the pan was v, the force displacing the pan upwards was mv. The continual deposition increased the weight of the pan and after a certain time t the pan returned to its original position, when

$$mv = mtg$$

where g is the acceleration due to gravity, assuming that all the sputtered atoms reaching the pan adhered to its surface. Hence the velocity v could be found from a time measurement only. The target and pan were kept at a high temperature to prevent mercury contamination. The average velocities for ejection normal to the target were for Ni, 6.5×10^5 cm/sec (12.7eV); W, 3.5×10^5 cm/sec (12eV) (5.5×10^5 cm/sec or 28eV for emission at 30° to the normal); Pt, 4×10^5 cm/sec (16eV); and (110) surface of monocrystalline Au, 3×10^5 cm/sec (9eV). The velocity was largely independent of ion energy over the range used: 600 to 900eV for Ni and W and 200 to 900eV for Pt and Au.

The second method[84] required the measurement of the forces on an ion-bombarded electrode in a mercury pool discharge plasma. Ions bombarding a target exert no net force, since the attraction of the target by an ion crossing the sheath is exactly balanced by the

impulse exerted by the ion when it hits the target. Forces can arise, however, due to rebounding neutralised ions, sputtered neutral atoms and due to radiometer forces. The latter were kept small by using gas pressures of less than 0.2μ. The target was in the form of a metal vane suspended from a quartz fibre torsion balance. One side of the vane was covered with quartz paper to keep the force on that side small and constant. Force curves versus energy were obtained for 22 metals for ion energies of 20 to 300eV. The force curves for clean metals closely resembled the corresponding yield curves, indicating that the forces were due to sputtering. From the yield curves, and approximating the angular distribution of sputtered atoms with a cosine law, the average velocities v of sputtered atoms could be calculated using the formula

$$v = \frac{3 \times 10^8}{2AS} F$$

where v is the velocity in cm/sec, F is the force in dynes/mA, [redacted] A is the atomic weight and S is the sputtering yield. The average velocities over the range 100 to 300eV were, for Cu, 3.1×10^5 cm/sec (3.3eV); Ag, 3.1×10^5 cm/sec (5.4eV); and Au, 2.2×10^5 cm/sec (5.1eV). For other metals the velocities were higher and in some cases increased to unbelievably high values as the energy was decreased.

9. MISCELLANEOUS EFFECTS OF SPUTTERING

9.1 Composition Changes of Alloys

It was reported by Asada and Quasebarth[85] that a copper cathode containing a trace of gold, when sputtered in a mercury glow discharge, became depleted in gold, due to preferential sputtering of the gold from the surface and its replenishment by diffusion from inside the cathode. However Fisher and Weber[86] found for alloys like brass and stainless steel, sputtered in a krypton glow discharge, that the sputtered deposits had the same composition as the original alloy.

Gillam[87] has sputtered thin sheets of Cu_3Au and observed the changes in the composition of the alloy by the transmission electron diffraction patterns. After bombardment with argon ions of up to 5keV energy the pattern consisted of doublets, showing that a layer of different composition had been formed. Initially the sputtering produced a layer more rich in gold than in Cu_3Au. Subsequent sputtering eroded three times as much Cu as Au. By using helium and xenon ions it was shown that the composition of the layer depended on both the ion and its energy. Similar effects were observed with other alloys.

9.2 Gas Clean-up

If a discharge is passed in a low pressure of inert gas it is frequently found that the gas pressure slowly decreases. It has

long been suspected that this phenomenon, which is known as gas clean-up, is connected with sputtering and the mechanism has recently been explained by the work of Blodgett and Vanderslice[88] and confirmed by Hall[89].

Clean-up occurs at any surface on which sputtered material is being deposited, by trapping gas atoms under the deposits. A small negative potential on the surface assists the clean-up by attracting positive ions which are then trapped. However, if the surface is sufficiently negative and the ion current density to it great enough to cause resputtering of the material, an equilibrium state is soon reached, after which no more gas is trapped. Hence clean-up does not occur at the cathode of a discharge as long as the ion current density is uniform (unless sputtered material is received at a greater rate from another electrode than it is being sputtered off).

Helium is an exception to the above mechanism, since sputtering is negligible at low ion energies. In this case clean-up does occur at the cathode, by penetration of atoms into the lattice[90]. Similarly, in Bayard-Alpert ion gauges sputtering is not important and clean-up occurs mainly by penetration of the surface layers of the glass, since the majority of the ions and metastables travel to the glass wall rather than to the electrodes.

10. THEORIES OF SPUTTERING

Sputtering theories fall into three classes: theories in which the momentum of the bombarding ion is considered to be transferred to the atoms of the target in a small number of separate two-body collisions between the ion and an atom and between two atoms, the total number of collisions considered being one, two, or three; theories in which a large number of collisions are considered; and the theory of evaporation of atoms from localized regions raised to a high temperature by the impact of the ions. The only evidence in support of the evaporation theory is the cosine angular distribution of sputtered material from polycrystalline targets at high energies (section 7.1). The angular distribution at low energies, and the deposit patterns from single crystals (section 7.2) can only be explained by collision theories. Also the high temperatures required by the evaporation theory would result in a much larger thermionic emission than that observed. In spite of these objections, the evaporation theory will be considered in some detail after the collision theories, since it was the basis for Townes'[17] theory of sputtering in the glow discharge.

10.1 Collision Theories Involving a Few Collisions

10.1.1 Early theories

Stark[91] assumed that for sputtering to occur the energy transferred from a normally incident ion to a target atom in an elastic

collision must be at least equal to the binding energy of the atoms. Hence the threshold energy for normal incidence is

$$V_o = \frac{(m+M)^2}{4mM} H \qquad (13)$$

where m is the mass of an ion, M is the mass of a target atom and H is the heat of sublimation in eV. (This notation will be used throughout the sections on sputtering theories). The values of V_o from this formula do not agree with sputtering experiments and it was not possible to obtain a formula for the yield. Also the "sputtered" atom would be driven into the lattice, not released from the surface!

Kingdon and Langmuir[31] considered the sputtering of thorium from a tungsten base as requiring two successive elastic impacts on the same target atom (see section 5.1). The resulting formula for the threshold energy was

$$V_o = \frac{(m+M)^4}{4mM(m-M)^2} H \qquad (14)$$

However if m and M are approximately equal, this formula gives very high values for V_o, which has never been observed.

10.1.2 Henschke's theory

Henschke[92] considered the bombarding ion as undergoing hard sphere elastic collisions with the target atoms, with energy losses

due to the excitation of Debye waves in the lattice during the collisions. The radii of the spheres were assumed to be determined by the largest closed electronic shells of the ion or atom. The threshold energies were calculated for three different collision mechanisms shown in Fig.28(a), (b) and (c).

Mechanism (a), in which the ion is obliquely incident on a surface atom, has threshold energy

$$V_o = \frac{(m+M)^2}{mM} H_{hkl} \frac{1}{(1+\delta)^2 \cos^2\gamma \cos^2 i} \qquad (15)$$

where i is the angle of incidence relative to the centre line between the ion and atom at the moment of impact, γ is the angle between the emission direction of the atom and the normal to the surface, H_{hkl} is the heat of vaporization for the appropriate surface crystal plane (hkl) and δ is the Debye wave dissipation coefficient. Lowest possible threshold occurs when

$$\cos(\gamma+i) = -\frac{c_\mu}{s}(1+\sin i)$$

where $c_\mu = c_m + c_M$, the sum of the collision radii of the ion and atom; and s is the separation of the rows of surface atoms.

Fig.28(b) shows the simplest case of sputtering by normally incident ions, requiring two collisions of the ion with target atoms.

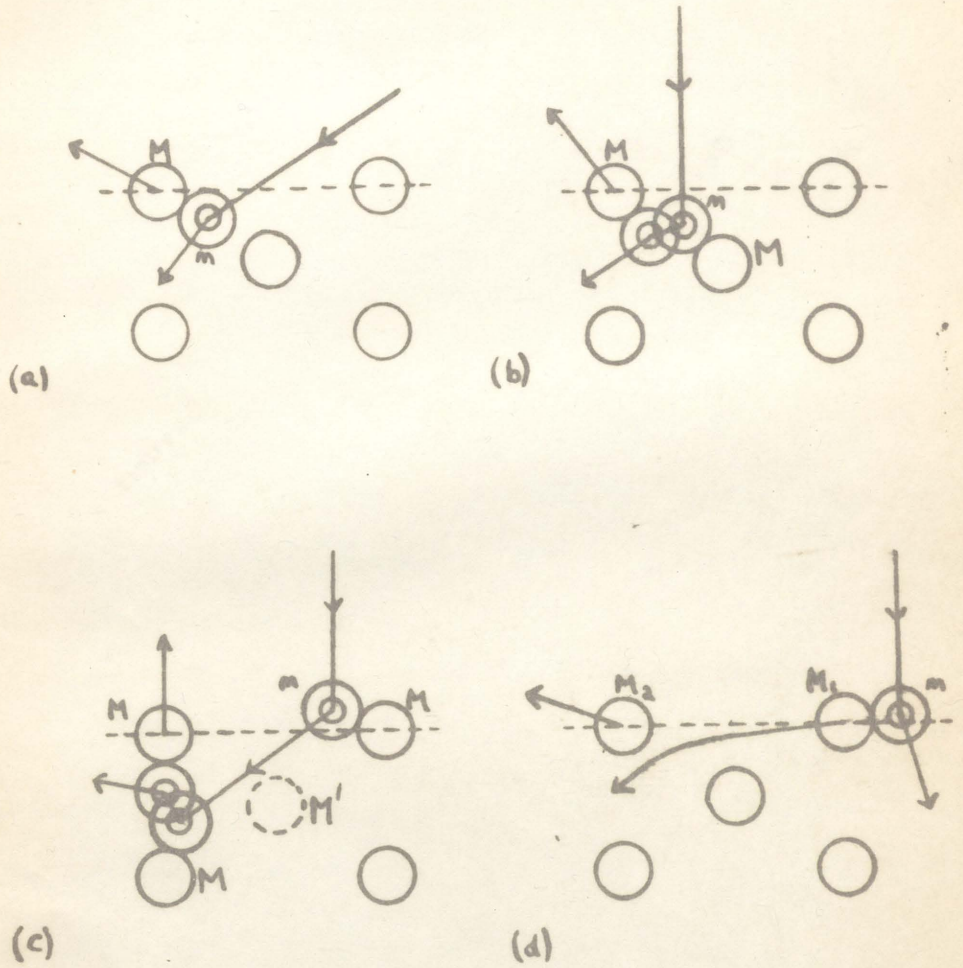

Fig.28. Collision mechanisms for sputtering: (a), (b) and (c) considered by Henschke; (d) considered by Langberg.

The first collision is with a "lower surface atom", which is assumed to have a very large effective mass since it is prevented from moving by the very large number of atoms behind it in the target. On rebound the ion hits an "upper surface atom", ejecting it obliquely. The threshold energy, which is greater than from equation (15), is

$$V_o = \frac{(m+M)^2}{m\,M} H_{hkl} \frac{1}{(1+\delta)^2 \cos^2\gamma \cos^2 i_2 \left[1-(1-\delta^2)\cos^2 i_1\right]} \qquad (16)$$

i_1 and i_2 being the angles of incidence for the first and second collisions.

In Fig.28(c) normally incident ions cause normal ejection of atoms after three collisions, requiring slightly higher energy still:

$$V_o = \frac{(m+M)^2}{m\,M} H_{hkl} \frac{1}{(1+\delta)^2 \cos^2\gamma \left[1-(1-\delta^2)\cos^2 i_2\right]\left[1-(1-\delta^2)\cos^2 i_1\right]} \qquad (17)$$

This mechanism can only occur after some of the upper surface atoms have been removed causing furrows in the lattice.

The quantities H_{hkl} have never been measured, and Henschke had to estimate them from the average values H for polycrystalline materials. The values of δ were found to be about 0.5 to 0.6 for b.c.c. metals and 0.4 to 0.5 for f.c.c., by comparing the theoretical values of V_o from equation (16) with Wehner's early threshold values.

By means of mechanisms (b) and (c), and allowing for the attenuating influence of the different electron densities in the ion paths within the lattice, Henschke[93] was able to completely explain the deposit patterns from single crystals. For instance, in sputtering the (110) plane of an f.c.c. crystal, mechanism (b) gives rise to the four outer spots whereas mechanism (c) explains the centre spot, which occurs at slightly higher energies.

For mechanism (b) Henschke[92] obtained a sputtering yield formula at low energies, by determining the ratio of the "favourable areas" for sputtering on the crystal surface to the total area, as a function of ion energy, and summing over the various crystal planes on the surface of a polycrystalline material. The result was

$$\left.\begin{aligned} S - S_m &= \frac{(V - V_o)^2}{2p} \quad \text{for } V \geqslant V_o \\ \text{and} \quad S &= 0 \quad \text{for } V < V_o \end{aligned}\right\} \qquad (18)$$

where the threshold value $V_o = \frac{2\pi C_M^2}{t}$ and $p = \frac{V_o}{s}$, s and t being constants for any one crystal plane but could vary somewhat with energy when averaged over all planes. S_m is the yield at the threshold energy V_o; i.e. the threshold is here defined as the lowest energy at which sputtering can be detected, not the energy at which the yield becomes zero. This equation can be compared with equation (7), which applied approximately at the lowest ion energies to Wehner's results, but differs from it because of S_m. Henschke found that, to fit his equation to Wehner's results for platinum in xenon over the range 34 to 200eV, several parabolae with different values of p were required.

Henschke calculated C_M, the collision radius of the target atom, from data on the radii of the largest closed electronic shells, for various elements. Since $V_0 = \frac{2\pi C_M^2}{t}$ he plotted C_M^2 multiplied by an arbitrary factor against atomic number and obtained good agreement with Wehner's threshold values (Fig.29). This is surprising owing to the approximate nature of these values, and the fact that other workers have obtained lower threshold values (section 5.5). The agreement, and the periodicity of the thresholds, is reduced if Wehner's more recent "cut-in" values are used[40].

10.1.3 Langberg's theory

Many other collision mechanisms are possible than the three considered by Henschke and Fig.28(d) shows that used by Langberg[94], for normally incident ions. An incoming ion collides with a surface atom (mass M_1), causing it to be displaced and collide with a second surface atom (mass M_2). This second collision, between two surface atoms, is considered, not as a collision between hard elastic spheres, but as under a Morse potential interaction; i.e. the potential energy $U(r)$ for two atoms at separation r is given by

$$U(r) = \phi\left\{\exp\left[a(d-r)\right] - 1\right\}^2$$

where ϕ is the energy to break the bond between the atoms, d is the equilibrium separation of the atoms and a is a lattice parameter

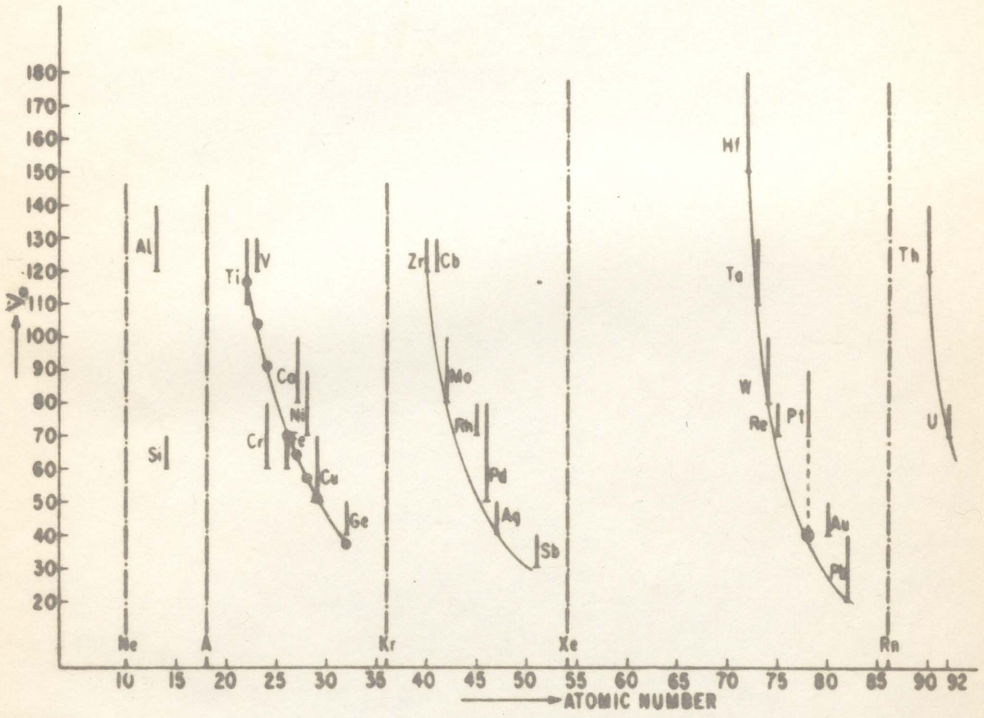

Fig.29. Periodicity of the threshold energies for various target elements bombarded with mercury ions, as determined by Wehner, compared with Henschke's theory.

related to compressibility. For the conditions shown in Fig.29(d), Conservation of energy and momentum indicate that the maximum energy stored in the second collision is

$$U(R) = \frac{M_2}{M_1+M_2}\,\eta_1 V \cos^2\alpha \left(1 - \frac{d^2\cos^2\alpha}{R^2}\right)$$

where V is the initial ion kinetic energy, $\eta_1 = \frac{4mM_1}{(m+M_1)^2}$ and R is the closest distance of approach of M_1 and M_2. The energy transfer conditions are optimized with respect to the recoil angle α of M_1 from the normal to the surface, after the first collision, by

$$\frac{\partial U(R)}{\partial(\cos^2\alpha)} = 0$$

giving the required value of α when

$$\cos^2\alpha = \frac{R^2}{2d^2}$$

Hence under optimum conditions of recoil

$$U(R) = \bar{U} = \frac{1}{4}\,\frac{M_2}{M_1+M_2}\,\eta_1 V \frac{R^2}{d^2}$$

The kinetic energy acquired by the second surface particle under optimum conditions can be shown to be

$$K = \frac{2\bar{U}}{\gamma}\,\frac{M_1}{M_1+M_2} = \frac{\eta_1\eta_2}{8\gamma} V \frac{R^2}{d^2}$$

where γ is approximately constant and equal to 0.63 and

$$\eta_2 = \frac{4M_1M_2}{(M_1+M_2)^2}$$

To sputter the second surface particle, tied by N bonds of energy ϕ, requires an escape energy of

$$\sigma N\phi = K = \frac{\eta_1\eta_2}{8\gamma} V \frac{R^2}{d^2}$$

where $\sigma \simeq 1{\cdot}1$ is due to the transfer of some kinetic energy to neighbouring atoms.

Hence, since the sublimation energy $H = \frac{n\phi}{2}$, where n is the number of nearest neighbours, the required ion energy is

$$V'' = \frac{16 H N d^2 \gamma \sigma}{n \eta_1 \eta_2 R^2}$$

To free the first particle its binding energy, on average equal to H, must be supplied, requiring ion energy

$$V' = \frac{H}{\eta_1 \cos^2\alpha} = \frac{2H d^2}{\eta_1 R^2}$$

From the Morse potential function $U(r)$, with $\phi = \frac{K}{N\sigma}$

$$\frac{R}{d} = 1 - \frac{1}{\alpha d} \ln\left\{1 + \left[\frac{N\sigma\gamma(M_1+M_2)}{2M_1}\right]^{\frac{1}{2}}\right\}$$

Hence the threshold energy for a lattice atom tied by N bonds is

$$V_N = V'' + V' = \frac{10H}{\eta_1}\left(1{\cdot}1\,\frac{N}{n} + 0{\cdot}2\right)\left[1 - \frac{1}{a\,d}\ln\left(1 + 0{\cdot}83\,N^{\frac{1}{2}}\right)\right]^{-2} \qquad (19)$$

assuming $M_1 = M_2$, $\eta_2 = 1$ and using the numerical values of γ and σ. It can be shown that the final direction of the second atom is such that it will in fact leave the surface.

A polycrystalline material, or a single crystal under ion bombardment in which many surface particles have been removed or knocked into interstitial positions, has surface atoms with numbers of bonds N varying from

$$N_a = N_o + N_1 + N_2$$

to

$$N_b = 1 + N_1 + N_2$$

where N_o is the maximum number of bonds to other surface atoms, one is the minimum number, and N_1 and N_2 are the numbers of bonds to the underlying first and second layers. The values of N_o, N_1 and N_2 for different crystal surfaces are given in Table 2 below, and the values of N_a and N_b for polycrystalline materials by selecting the lattice planes giving the largest and smallest number respectively. The values of n are also given.

Table 2

	F.c.c.				Hcp	B.c.c.			Diamond		
	(100)	(110)	(111)	(112)	(0001)	(100)	(110)	(111)	(100)	(110)	(111)
N_0	4	2	6	2	6	0	4	0	0	2	0 0
N_1	4	4	3	3	3	4	2	3	2	1	3 1
N_2		1		2				1			
N_a		9			9		6			3	
N_b		4			4		3			2	
n		12			12		8			4	

The yield S_N for particles tied by N bonds can be shown to be given by

$$S_N = P_N (V - V_N) \qquad \text{for } V \geqslant V_N$$

$$S_N = 0 \qquad \text{for } V \leqslant V_N$$

where P_N is a constant

Hence the total yield for values of N between N_b and N_a

$$= S = \sum_{N=N_b}^{N=N_a} P_N (V - V_N)$$

$$\simeq \int_{V_b}^{V_a} P(V_N)\,(V - V_N)\, d V_N$$

where V_a and V_b are the highest and lowest thresholds, corresponding to N_a and N_b

Assuming $P(V_N) = b =$ a constant for $V_b \leqslant V_N \leqslant V_a$

it is found that

$$\left.\begin{aligned} S &= 0 && \text{for } V \leqslant V_b \\ S &= \tfrac{1}{2} b (V - V_b)^2 && \text{for } V_b \leqslant V \leqslant V_a \\ S &= b(V_a - V_b)\left[V - \tfrac{1}{2}(V_a + V_b)\right] && \text{for } V \geqslant V_a \end{aligned}\right\} \qquad (20)$$

Equations(20) for the yield are seen to be of the same form as equations (7) and (9) which cover the two low energy ranges. The threshold energy $V_o = V_b$ and the "cut-in" energy $V_1 = \frac{1}{2}(V_a + V_b)$.

V_a can be identified with the "ankle" energy.

The equations were fitted to Wehner's platinum-mercury results by suitably choosing the value of b,

with $V_o = V_b = 54.7\,eV$, $V_1 = 85.6\,eV$ and $V_a = 116\,eV$.

Fig.15 shows the curve drawn through the experimental points.

Wehner's early threshold values tended to lie between the calculated values of V_o and V_1. It was shown that Wehner's threshold law (equation (8)) could be expressed as

$$V_o = \frac{H}{\eta_1} \frac{C}{(ad)^2} \qquad (21)$$

with $C = 187$ for f.c.c. and h.c.p. lattices and $C = 167$ for b.c.c. lattice, whereas the calculated thresholds V_a, V_o and V_i could be expressed by an approximated form of equation (19):

$$V_N = \frac{H}{\eta_i}\left[A_N + \frac{B_N}{(a\,d)^2}\right] \qquad (22)$$

where A_N and B_N are constants. Fig.30 shows the effect of plotting $\frac{V_N \eta_i}{H}$ versus $(a\,d)^{-2}$ for the three calculated thresholds and compares them with Wehner's results, for f.c.c. and h.c.p. lattices. It will be noticed that Wehner's results nearly all fall between the lines for V_o and V_i

Langberg's theory seems to be the most satisfactory of those involving only a few collisions, particularly as it derives the yield equation for both the two low energy regions (equations (7) and (9)) and has no adjustable constants in the threshold equation, but it is possible that Henschke's collision mechanism (b) might be the more appropriate for the lowest energies. Unfortunately the Henschke threshold equations have an unknown constant δ and the yield equation (18) differs somewhat from the experimental equation (7). It will be noticed that the threshold equations from most of the theories (equations (13), (15), (16), (17) and (19)) are similar to Wehner's "cut-in" equation (10) with different values for the constant B. Wehner is believed to have replaced his earlier threshold law

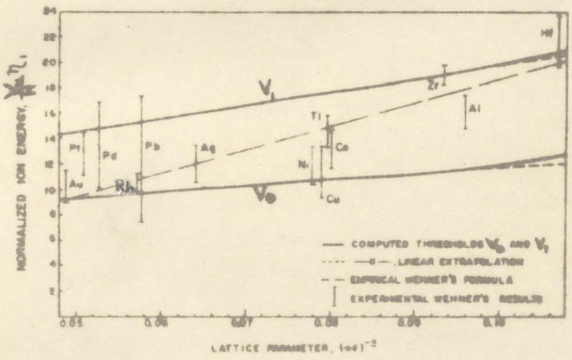

Fig.30. Normalized threshold energies of f.c.c. and h.c.p. metals sputtered by mercury ions, as determined by Wehner, compared with Langberg's theory.

(equation (8)) by this equation since the former was reduceable to equation (21), which was similar to a simplified form of equation (19) (equation (22)).

10.2 Collision Theories Involving Many Collisions

10.2.1 Neutron cooling and radiation damage theory (Keywell)

The theory of sputtering based on that of neutron cooling, due to Keywell[53], which is somewhat older than the theories of Henschke and Langberg, may be applicable at moderately high energies. If an ion of energy V retains a fraction of its energy $e^{-\xi}$ after collision with an atom of the "moderator" then after n collisions it has energy

$$V_n = V e^{-n\xi}$$

If one atom is sputtered per collision then the yield is

$$S = n = \frac{1}{\xi} \ln \frac{V}{V_n} \qquad (23)$$

where V_n, the energy after n collisions, is an energy less than the threshold and ξ is given by the expression

$$\xi = 1 - \frac{(M-m)^2}{2Mm} \ln\left(\frac{M+m}{M-m}\right)$$

Equation (23) can be compared with equation (12) and Fig.20 shows equation (23) applied to Keywell's results for silver sputtered by argon, for which $\xi = 0.59$, taking $V_n = 39$ volts.

The theory as given above only applies to heavy ions like argon. In order to extend it to lighter ions, Keywell considered the fast moving atoms produced by the ion bombardment to release other atoms by radiation damage. The average fractional energy transferred to an atom at the nth collision of the ion

$$= \epsilon = \frac{2mM}{(m+M)^2} = \frac{\eta}{2}$$

Hence the energy of the $(n+1)$ th recoil atom

$$= \bar{V}_{n+1} = \epsilon V_n = \epsilon V e^{-n\xi}$$

The number of displacements due to atom of energy $\bar{V}$ in a metal of displacement energy V_d was taken as

$$n_s = \left(\frac{\bar{V}}{V_d}\right)^{\frac{1}{2}}$$

The number of displaced atoms formed at depth x below the surface, escaping from the surface, was assumed to be

$$n_e = e^{-\beta x} n_s$$

where β is a constant. The depth x was assumed to be determined by the ion progressing by a random walk, so that

$$x = k n^{\frac{1}{2}}$$

where k is a constant.

Hence the yield $= S = \sum_{n=1}^{n_c} n_e = \left(\frac{\epsilon V}{V_d}\right)^{\frac{1}{2}} \sum_{n=1}^{n_c} e^{-\alpha n^{\frac{1}{2}}} e^{-(n-1)\frac{\delta}{2}}$

where $\alpha = k\beta$ and $n_c = \frac{1}{\delta} \ln \frac{V}{V_n}$ is the number of collisions made by the ion. For $m < M$ a correction was necessary for the fact that some of the incident ions rebound from the surface at the first collision. If the probability of penetration is f_p and of rebound $f_r = 1 - f_p$, the yield equation becomes

$$S = \left(\frac{\epsilon V}{V_d}\right)^{\frac{1}{2}} \sum_{n=1}^{n_c} \left(f_p + 1.32\, \delta f_r\right) e^{-\alpha n^{\frac{1}{2}}} e^{-(n-1)\frac{\delta}{2}} \qquad (24)$$

where $n_c = \frac{1}{\delta} \ln \frac{V}{V_n}$ and $\delta = 0$ for $n \neq 1$

$\delta = 1$ for $n = 1$

Equation (24) bears some resemblance to equation (6) which applies at high energies. Keywell fitted equation (24) to his results for various gas and metal combinations, as shown in Fig.21 for silver, but the fit appears to be less satisfactory for argon than that for equation (23).

10.2.2 Neutron diffusion theory (Harrison)

Harrison[95],[96],[97] produced a theory based on that of neutron diffusion, in which all particles not in thermal equilibrium

with the lattice were described by a gas-like model in which the atoms moved with constant mean free path. Collisions were assumed to occur only with "fixed" lattice atoms, but binding energies were neglected. The expression for the yield depended upon four atomic parameters of the system of which only one could be measured with precision. The expression for the yield, which requires a long proof and is difficult to apply in practice, is

$$S = R_0 \sum_{n=1}^{4} R_n \left[\left(\frac{V}{V_0} \right)^{t_n} - 1 \right] \qquad (25)$$

where V_0 is the threshold energy and R_0, R_n and t_n are constants which are, in principle, calculable. The theory was fitted to Keywell's results[95],[96] and proved rather more satisfactory than Keywell's own theory, probably due to the fact that with only one of the four atomic parameters capable of accurate measurement, there would be three adjustable constants. At low energies equation (25) could be reduced to equation (9)[97]. Recently Harrison[64] seems to be adapting his theory to include the Silsbee[98] chain mechanism, described below.

10.2.3 Silsbee's chain theory

In explaining the deposit patterns from single crystals Wehner[35] suggested that a shock wave is initiated from the place of impact of the ion, the energy travelling most efficiently along the

close-packed directions in the lattice, until a small part of the energy reaches a surface atom. If this energy is sufficient to overcome the binding energy of the surface atom the latter may be sputtered. This transfer of energy along chains of close-packed atoms is very similar to the well-known experiment of allowing a billiard ball to move along the axis of a row of billiard balls in contact, to hit the first ball in the row. Momentum is transferred from ball to ball down the row, but only the last ball shows appreciable displacement.

Silsbee[98] showed that if the incoming particle was incident at an angle β to the axis of a chain of atoms, then the angles at which successive atoms moved would decrease until the motion was entirely along the chain, i.e. the momentum would be focused along the chain, provided

$$\cos\beta > \frac{d}{2r}$$

where d is the separation of the centres of the atoms and r is their diameter. Under these conditions the transfer of energy along the chain is very efficient, and this mechanism is considered to be important in the explanation of sputtering and radiation damage.

Harrison and Magnuson[99] have suggested that because of the chain mechanism, sublimation from a solid at temperatures well below the melting point, e.g. from copper at room temperature, might show

a spot deposit pattern. The experiment would, however, probably require a millenium for completion. In spite of this suggestion of a similarity between sublimation and sputtering, Harrison and Magnuson went on to calculate sputtering thresholds using a theory based on the chain mechanism and obtained values of the order of, or lower than, those of Morgulis and Tishchenko, i.e. much lower than Wehner's experimental or Langberg's theoretical values. The lowest calculated threshold was 1.16eV for antimony sputtered by argon, for which the Morgulis and Tishchenko value is 3eV. However it seems that since experimental thresholds are becoming lower and lower, and if sublimation is similar to sputtering and can be considered as sputtering at zero ion energy, then it is quite likely that there is no definite threshold.

The Langberg threshold values correspond to the energy at which sputtering first becomes appreciable; at lower energies sputtering may be due to atoms which happen to be very loosely bound to the surface or may even be near to sublimating. The Langberg theory would give very low threshold values if atoms were considered for which $N=1$. The Langberg and Henschke theories can, of course, be considered as involving simplified chain mechanisms requiring only the surface atoms, and should be adequate for low ion energies, but the chain mechanisms would be required for a rigorous theory of sputtering.

Harrison[64] has suggested that the "ankle" energy, i.e. the energy at which the yield curve changes from equation (7) to equation (9),

which corresponds to Langberg's V_a , is the maximum energy propagated along a chain of close-packed atoms.

10.3 Evaporation Theory of Sputtering, and Sputtering in the Glow Discharge (Townes)

The evaporation theory of sputtering of von Hippel[100],[101] was developed by Townes[17], whose treatment is given here.

An ion is assumed to deliver its energy V almost instantaneously to a small hemispherical region of radius r_o . If the energy is propagated as heat an approximate solution for the temperature T at distance r from the centre of the impact region and time t after the impact is

$$T = \frac{1.7 \times 10^{-21}}{\rho s \left(\frac{ct}{\rho s}\right)^{3/2}} V \exp\left(\frac{-r^2 \rho s}{4ct}\right) + T_o \qquad \text{if } \frac{ct}{\rho s} > r_o^2$$

where T_o is the temperature before the collision and ρ, s and c are respectively the density, specific heat and conductivity of the cathode material.

The vapour pressure of the cathode material was assumed to be

$$p = \exp\left(b - \frac{a}{kT}\right)$$

where k is Boltzmann's constant and a and b are constants for the cathode material. The number of molecules leaving unit area per second is

$$\nu = \frac{C_2 p}{M v}$$

where M is the molecular mass, v the average velocity of molecules in the vapour state and C_2 the fraction which stick to the collecting surface on impact. Hence

$$\nu = \frac{C_2 \exp\left(b - \frac{a}{kT}\right)}{2\left(\frac{2}{\pi} M k T\right)^{\frac{1}{2}}}$$

The sputtering yield was obtained by multiplying the maximum evaporation rate by the time for the temperature to fall to a value such that the evaporation rate is halved, and the area over which the evaporation is greater than half maximum, giving, on neglecting T_0,

$$S = \frac{1.5 \times 10^{-55} C_2 V^{3/2}}{a^2 c^{5/4} (\rho s t_0)^{1/4} M^{1/2}} \exp\left[b - \frac{a (c t_0)^{3/2}}{2.3 \times 10^{-37} V (\rho s)^{1/2}}\right] \qquad (26)$$

where t_0 is the time required for the collision. However with $V = 8eV$, this gave $S = 2$, for barium sputtered by argon, which is ridiculously high, although Townes considered it reasonable.

In order to apply this to sputtering in the glow discharge, Townes calculated the energy distribution of the ions hitting the cathode,

by the following method. Consider a typical ion in an electric field E, starting from rest and having a mean free path in the gas λ. After moving in the direction of the field an average distance λ, it will have energy $E\lambda$, and will then collide with a molecule of approximately the same mass as the ion. The average energy after the collision will be $\frac{1}{2}E\lambda$, most of the momentum being in the direction of E, and so the energy before the next collision is $E\lambda + \frac{1}{2}E\lambda$. Hence after n collisions the average energy is

$$\bar{V} = E\lambda + \tfrac{1}{2}E\lambda + \text{------} \left(\tfrac{1}{2}\right)^{n} E\lambda \simeq 2E\lambda$$

[redacted] assuming E is constant over several mean free paths. This is an upper limit for $\bar{V}$ since not all of the ionic velocity is in the field direction. By considering variations in the energy contributions of only the last two free paths, Townes showed that the number of ions having energy less than V was given approximately by the expression

$$\frac{dn(V)}{dV} = \frac{n_0}{E\lambda} \exp\left(-\frac{V}{E\lambda} + \frac{1}{2}\right)\left[\frac{9}{8} + \frac{V}{4E\lambda} - \exp\left(\frac{V}{E\lambda} + \frac{1}{2}\right)\right]$$

where n_0 is the total number of ions.

The electric field E at distance x from the cathode was assumed to be given by

$$E = E_c\left(1 - \frac{x}{d_c}\right)$$

where d_c is the length of the dark space and E_c is the field at the cathode. Hence it may be shown that

$$E_c = 2\left[\frac{\pi j V_c}{(1+\gamma) k}\right]$$

where j is the current density at the cathode, V_c is the cathode fall of potential, γ is the secondary electron coefficient and k is the ionic mobility.

Putting $\lambda = \frac{\Lambda}{p}$ and $k = \frac{K}{p}$, where K is assumed to be given by the expression $K = \frac{K}{\sqrt{V}}$, and p is the gas pressure, then

$$E_c \lambda = 2\left[\frac{2\pi \Lambda^3}{(1+\gamma) K}\right]^{2/5}\left(\frac{V_c j}{p^2}\right)^{2/5}$$

The motion of sputtered material through the gas was assumed to occur by a diffusion process. For the case of the cathode and collector of sputtered material being parallel planes separated by a distance d, the number of atoms deposited per second on the collector was

$$J = \frac{\pi J_o \lambda}{2 C_1 d} \ll J_o$$

where C_1 is the fraction of the atoms which, having returned to the cathode, adhere to it and J_o is the number of atoms emitted from the

cathode in unit time (proportional to the rate of sputtering M as defined in section 1.1) given by

$$J_o = \int_{V_o}^{\infty} \frac{dJ_o}{dn} \frac{dn}{dV} dV$$

where V_o is the energy required to release one atom from the cathode surface and

$$\frac{dJ_o}{dn} = S$$

Hence the following approximate expressions were obtained for J :

$$\left.\begin{aligned} &\text{If } E\lambda \gg V_o, \quad J = \frac{A\,i}{p}\left(\frac{V_c\,j}{p^2}\right)^{3/5} \\ &\text{If } E\lambda \ll V_o, \quad J = \frac{B\,i}{p}\exp\left[(-cV_o)\left(\frac{p^2}{V_c j}\right)^{2/5}\right]\left[\frac{cV_o}{4}\left(\frac{p^2}{V_c j}\right)^{2/5} + \frac{7}{4}\right] \end{aligned}\right\} \quad (27)$$

where i is the total discharge current, A and B are constants and

$$c = \frac{1}{2}\left[\frac{(1+\gamma)K}{2\pi\Lambda^3}\right]^{2/5}$$

The first expression depends entirely on the yield function, and not the distribution of ion energies, and was expected to be less accurate than the second, which depends mainly on the energy distribution function. A simplified version of the second expression, in the form

$$J = a\,i\,e^{-\frac{b}{i^{2/5}}}\left(7 + \frac{b}{i^{2/5}}\right)$$

where a and b are adjustable constants, was applied to Rockwood's results (see section 2.1) and Fig.7 shows the theoretical line drawn through the experimental points. It will be noticed that the line does not really curve quite sufficiently to fit the points adequately. One inconsistency in Townes' paper is the statement that the theory should be more reliable in 99% neon - 1% argon, in which a discharge consists essentially of argon ions moving in neon gas, than in pure argon, where charge transfer makes the ionic mean free path strongly dependant on ionic velocity. However, the expression for the energy distribution function was derived on the assumption of equal atomic and ionic mass, although it could of course be adapted for unequal masses. There are also a number of misprints in the mathematical expressions, which have been corrected here.

The theory is too inaccurate to justify the use of the complicated expressions (27). No allowance was made for the effect of the angular distribution of the ions incident on the cathode. There is no experimental evidence for the derived yield function equation (26) but this could be replaced by some other expression, such as equation (7). However this will have little effect in high pressure discharges, for which $E\lambda \ll V_o$.

The problem of the diffusion of sputtered material through the gas has been considered theoretically in some detail by Ecker and

Emeléus[102], for a cylindrical discharge tube with plane parallel electrodes perpendicular to the axis of the tube and extending to the walls. They showed that, because the emission velocity of the sputtered atoms is much greater than the equilibrium velocity in the gas, the concentration of sputtered atoms passes through a maximum in front of the cathode, and they confirmed that the majority of the sputtered atoms diffuse back to the cathode.

11. CONCLUSION

A number of discrepancies exist between the results of various workers, which have been described. Firstly there is the question as to whether or not there is a threshold energy. As more sensitive methods of detecting sputtering are used so the threshold energies become lower. It has been suggested that there is no threshold energy, sputtering simply merging into the background sublimation at low energies (section 10.2.3). The energies V_o and V_1 in equations (7) and (9) indicate where the sputtering becomes appreciable, but not the lowest energies for sputtering. Below V_o the sputtering is probably due to the few loosely bound atoms on the target surface.

Secondly a discrepancy exists regarding sputtering in helium, some workers finding none whereas others observed it at quite low energies, e.g. Morgulis and Tishchenko (Fig.18). The explanation is probably the presence of impurities causing sputtering, in many cases, but as regards Morgulis and Tishchenko it may be the use of a very sensitive detector of sputtering. Much more experimental work must be carried out in helium.

A rigorous theory of sputtering will probably require the Silsbee chain mechanism and Harrison appears to be attempting to obtain such a theory. However the Langberg or Henschke theories appear

to be quite adequate at low energies. It is unlikely that an accurate theory of sputtering in the glow discharge will be obtained since it must combine a theory of sputtering, a theory of the glow discharge, and a diffusion theory for the sputtered material in the gas.

12. REFERENCES

1.	Grove, W.R.	Phil. Trans Roy. Soc 142, 87 (1852).	See ref(6)
2.	Pluecker, J.	Pogg. Ann. 103, 88 (1858); 105, 67 (1858)	See ref(6)
3.	Oliphant, M.L.E.	Proc. Roy. Soc. A124, 228 (1929).	
4.	Jacob, L.	Nature 157, 586 (1946)	
5.	Johnson, E.A. & Harris L.	Phys. Rev. 45, 630 (1934)	
6.	Massey, H.S.W. & Burhop, E.H.S.	"Electronic and Ionic Impact Phenomena", p.578, (Oxford Univ. Press, 1952)	
7.	Francis, G.	"Encyclopaedia of Physics" Vol.22, p.154 (Springer-Verlag, 1956)	
8.	Wehner, G.K.	"Advances in Electronics and Electron Physics", Vol.7, p.239 (Academic Press Inc. New York, 1955)	
9.	Ditchburn, R.W.	Proc. Roy. Soc. A141, 169 (1933)	
10.	Guentherschulze, A.	Z. Phys. 38, 575 (1926)	
11.	Guentherschulze, A. & Tollmien, W.	Z. Phys. 119, 685 (1942)	
12.	Guentherschulze, A.	Z. Phys. 119, 79 (1942)	
13.	Guentherschulze, A.	Vacuum 3, 360 (1953)	
14.	Guentherschulze, A.	Z. Phys. 118, 145 (1941)	
15.	Seeliger, R.	Z. Phys. 119, 482 (1942)	
16.	Rockwood, G.H.	Trans Amer. Inst. Elect. Engrs 60, 901 (1941)	
17.	Townes, C.H.	Phys. Rev. 65, 319 (1944)	
18.	Stocker, B.J.	Brit. J. Appl. Phys. 12, 465 (1961) Reprint enclosed.	
19.	Von Hippel, A.	Ann. Phys. 80, 672 (1926)	

20. Baum, T. Z. Phys. 40, 686 (1927)

21. Cayless, M.A. & Forster-Brown, A.D. Brit. J. Appl. Phys. 8, 380 (1957)

22. Guentherschulze, A. Z. Phys. 36, 563 (1926)

23. Holland, L. & Siddall, G. Vacuum 3, 375 (1953)

24. Penning, F.M. & Moubis, J.H.A. Philips Res. Rep. 1, 119 (1946)

25. Jurriaanse, T., Penning, F.M. & Moubis, J.H.A. Philips Res. Rep. 1, 225 (1946)

26. Penning, F.M. & Moubis, J.H.A. Physica 15, 721 (1949)

27. Jurriaanse, T. Philips Techn. Rev. 8, 272 (1946)

28. McCutcheon, D.M. J. Appl. Phys. 20, 414 (1949)

29. Penning, F.M. & Moubis, J.H.A. Proc. K. Ned. Akad. Wetensch. 43, 41 (1940)

30. Research Staff of the G.E.C., London Phil. Mag., Series 6, 45, 98 (1923)

31. Kingdon, K.H. & Langmuir, I. Phys. Rev. 22, 148 (1923)

32. Guentherschulze, A. & Meyer, K. Z. Phys. 62, 607 (1930)

33. Meyer, K. & Guentherschulze, A. Z. Phys. 71, 279 (1931)

34. Wehner, G.K. and Medicus, G. J. Appl. Phys. 25, 698 (1954)

35. Wehner, G.K. Phys. Rev. 102, 690 (1956)

36. Wehner, G.K. Phys. Rev. 108, 35 (1957)

37. Wehner, G.K. Phys. Rev. 112, 1120 (1958)

38. Wehner, G.K. Phys. Rev. 93, 633 (1954)

39. Hagstrum, H.D. — Phys. Rev. 96, 336 (1954)

40. Henschke, E.B. — Phys. Rev. 121, 1286 (1961)

41. Laegreid, N., Wehner, G.K. & Meckel, B. — J. Appl. Phys. 30, 374 (1959)

42. Laegreid, N. & Wehner, G.K. — J. Appl. Phys. 32, 365 (1961)

43. Stuart, R.V. & Wehner, G.K. — Phys. Rev. Letters 4, 409 (1960)

44. Morgulis, N.D. & Tishchenko, V.D. — Soviet Phys. - J.E.T.P. 3, 52 (1956)

45. Morgulis, N.D. & Tishchenko, V.D. — Bull. Acad. Sci. U.S.S.R. Phys. Ser. 20, 1082 (1956)

46. Strachan, J.F. & Harris, N.L. — Proc. Phys. Soc. B69, 1148 (1956)

47. Wolsky, S.P. — Phys. Rev. 108, 1131 (1957)

48. Wolsky, S.P. & Zdanuk, E.J. — Phys. Rev. 121, 374 (1961)

49. Wolsky, S.P. & Zdanuk, E.J. — J. Appl. Phys. 32, 782 (1961)

50. Koedam, M. — Thesis, Utrecht, March 1961 Reprinted in Philips Res. Rep. 16, 101(1961) 16, 266(1961)

51. Weijsenfeld, C.H. Hoogendoorn, A. & Koedam, M. — Physica 27, 763 (1961)

52. Timoshenko, G. — J. Appl. Phys. 12, 69 (1941)

53. Keywell, F. — Phys. Rev. 87, 160 (1952)

54. Keywell, F. — Phys. Rev. 97, 1611 (1955)

55. Bradley, R.C. — Phys. Rev. 93, 719 (1954)

56. Yonts, O.C., Normand, C.E. & Harrison Jr., D.E. — J. Appl. Phys. 31, 447 (1960)

57. Grönlund, F. & Moore, W.J. — J. Chem. Phys. 32, 1540 (1960)

58. Rol. P.K. Fluit, J.M. & Kistemaker, J. — Physica 26, 1000 (1960)

59. Alméri, O. & Bruce, G. — Nucl. Instr. and Meth. 11, 257 (1961) 11, 279 (1961)

60. Yonts, O.C. & Harrison, Jr. D.E. — J. Appl. Phys. 31, 1583 (1960)

61. Wehner, G.K. & Rosenberg, D. — J. Appl. Phys. 32, 887 (1961)

62. Hines, R.L. & Waller, R. — J. Appl. Phys. 32, 202 (1961)

63. McKeown, D. — Rev. Sci. Instr. 32, 133 (1961)

64. Harrison, Jr. D.E. — J. Appl. Phys. 32, 924 (1961)

65. Fetz, H. — Z. Phys. 119, 590 (1942)

66. Wehner, G.K. — J. Appl. Phys. 25, 270 (1954)

67. Wehner, G.K. — J. Appl. Phys. 30, 1762 (1959)

68. Molchanov, V.A. & Tel'kovskii, V.G. — Soviet Phys-Doklady 6, 137 (1961)

69. Rol, P.K., Fluit, J.M. Viehböck, F.P. & de Jong, M. — Proc. 4th Int. Conf. on Ionis. Phenomena in Gases, Uppsala, 257 (1959)

70. Molchanov, V.A. Tel'kovskii V.G. & Chicherov, V.M. — Soviet Phys. - Doklady 6, 222 (1961)

71. Seeliger, R. & Sommermeyer, K. — Z. Phys. 93, 692 (1935)

72. O'Briain, C.D., Lindner, A. & Moore, W.J. — J. Chem. Phys. 29, 3 (1958)

73.	Cobić, B. & Perović, B.	Proc. 4th Int. Conf. on Ioniz. Phenomena in Gases, Uppsala, 260 (1959)
74.	Wehner, G.K. & Rosenberg, D.	J. Appl. Phys. 31, 177 (1960)
75.	Stein, R.P. & Hurlbut, F.C.	Phys. Rev. 123, 790 (1961)
76.	Wehner, G.K.	J. Appl. Phys. 26, 1056 (1955)
77.	Anderson, G.S. & Wehner, G.K.	J. Appl. Phys. 31, 2305 (1960)
78.	Yurasova, V.E. Pleshivtsev, N.V. & Orfanov, I.V.	Soviet, Phys. - J.E.T.P. 10, 689 (1960)
79.	Magnuson, G.D. Meckel B.B. & Harkins P.A.	J. Appl. Phys. 32, 369 (1961)
80.	Honig, R.E.	J. Appl. Phys. 29, 549 (1958)
81.	Bradley, R.C.	J. Appl. Phys. 30, 1 (1959)
82.	Stanton, H.E.	J. Appl. Phys. 31, 678 (1960)
83.	Wehner, G.K.	Phys. Rev. 114, 1270 (1959)
84.	Wehner, G.K.	J. Appl. Phys. 31, 1392 (1960)
85.	Asada, T. & Quasebarth, K.	Z. Phys. Chem. A143, 435 (1929)
86.	Fisher, T.F. & Weber, C.E.	J. Appl. Phys. 23, 181 (1952)
87.	Gillam, E.	J. Phys. Chem. Solids 11, 55 (1959)
88.	Blodgett, K.B. & Vanderslice, T.A.	J. Appl. Phys. 31, 1017 (1960)
89.	Hall, R.F.	J. Electronics & Control 11, 101 (1961)
90.	Carmichael, J.H. Trendelenburg, E.A.	J. Appl. Phys. 29, 1570 (1958)

91.	Stark, J.	Z. Electrochem. 14, 752 (1908) 15, 509 (1909)
92.	Henschke, E.B.	Phys. Rev. 106, 737 (1957)
93.	Henschke, E.B.	J. Appl. Phys. 28, 411 (1957)
94.	Langberg, E.	Phys. Rev. 111, 91 (1958)
95.	Harrison, Jr., D.E.	Phys. Rev. 102, 1473 (1956)
96.	Harrison, Jr. D.E.	Phys. Rev. 105, 1202 (1957)
97.	Harrison, Jr. D.E.	J. Chem. Phys. 32, 1336 (1960)
98.	Silsbee, R.H.	J. Appl. Phys. 28, 1246 (1957)
99.	Harrison, Jr. D.E. & Magnuson, G.D.	Phys. Rev. 122, 1421 (1961)
100.	Von Hippel, A.	Ann. Phys. 81, 1043 (1926)
101.	Blechschmidt, E. & von Hippel, A.	Ann. Phys. 86, 1006 (1928)
102.	Ecker, G. & Emeléus, K.G.	Proc. Phys. Soc. B67, 546 (1954)